April 2017

Flexible Solar Cells

Edward Robert Peglow
Worcester Polytechnic Institute

Francis Joseph LaRovere
Worcester Polytechnic Institute

Michael James McMahon
Worcester Polytechnic Institute

Flexible Solar Cells

A Major Qualifying Project Submitted to the Faculty

Of Worcester Polytechnic Institute

In Partial Fulfillment of the requirements for the

Degree in Bachelor of Science

In

Mechanical Engineering

By

Francis LaRovere

Edward Peglow

Michael McMahon

Project Advisor

Professor Pratap Rao, Advisor

Table of Contents

Table of Figures

Table of Tables

Acknowledgments

We would like to acknowledge all the help that we received from our advisor, Professor Pratap Rao. We would also like to thank Binod Giri, Zhehao Zhu, Lite Zhou, and Yang Yang, for their help in lab.

Abstract

Solar energy can be made more widely accessible by creating versatile solar cells that can be implemented in novel applications. Making solar cells mechanically flexible greatly increases their versatility. Current materials being used for flexible solar cells are unstable, expensive, inefficient, or toxic. The goal of our project was to synthesize flexible absorber, buffer, and blocking layers out of earth-abundant, non-toxic materials to achieve solar cells that are both flexible and efficient. We chose antimony sulfide (Sb_2S_3), copper (I) thiocyanate (CuSCN) and titanium dioxide (TiO_2) for these respective layers on the basis of efficiency, mechanical flexibility, cost, stability and safety. We explored low-temperature synthesis methods to realize this flexible design on a plastic substrate, and evaluated the design by observing the microstructural changes that occurred due to bending.

1. Introduction

Mechanically flexible solar cells could drastically change the way energy is generated in the future. Some of the applications include use in high altitude and space environments for telecommunication purposes, integrated cells for building energy, use as the primary energy source in soft robotics, and even on clothing to charge a smartphone. To create a more flexible solar cell there needs to be a compromise between thickness, mechanical resilience, and durability.

Efforts in advancing the technology of solar cell devices have been primarily concerned with cost and efficiency of the cells. High device cost and preparation required to fabricate inorganic solar cells, which are most frequently used, have limited the overall impact that solar energy can have. The most common inorganic solar cell type is made using crystalline silicon as the semiconductor layer, which is separated into two layers of different types, positive and negative (p and n). The semiconductor layer of this cell is sandwiched between a top cathode and bottom anode layer, where the cathode has metal connections placed onto it and the anode layer is attached to a metal contact, so that the cell can be wired into a circuit. This basic construction is constant for all major cell types, including CdTe, CIGS, CIS, dye sensitized, polymer, and perovskite cells. Because of how broad improving cost and effectiveness is for making better solar cells, many avenues of composition and construction have been researched for all cell types.

An alternative way of making solar more widely accessible is to create a versatile solar cell that can be implemented in more places. The inorganic solar cells we created is a type of thin film solar cell that can be used in mechanically flexible applications, creating further options where solar cells can be used. Furthermore, because our cell is completely inorganic it has increased stability. This type of solar cells differs from silicon solar cells first in that the cell layers are constructed using deposition, creating a thinner, lighter, and as previously stated flexible cell. Secondly this cell type is different because the p and n type layer are made from different classes of material, with the p-type being organic and the n-type inorganic. This helps to create a simpler cell construction overall which aids in creating a more flexible device. Although much research has been done on improving the semiconductor layer, changes to the other layers in the cell structure have been considered less thoroughly and can likely be improved to increase flexibility and efficiency.

2. Scope

This report herein will detail the steps taken to create a solar cell where the main goal is flexibility, rather than efficiency or cost. The general construction of the cell will be an inorganic hybrid heterojunction solar cell, where the basic layering of the cell will be (PET/Glass)/ITO/TiO_2/Sb_2S_3/CuSCN/(Au/Pd)

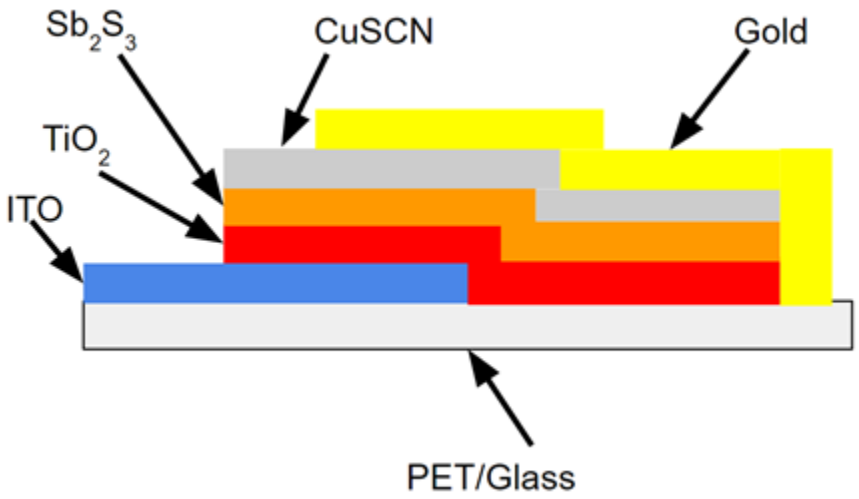

Figure 1 Final Cell Layout

In this structure, the study will center around the effects that cell layers have on flexibility and efficiency, by modifying the ZnO layer and changing what is used as the n-type semiconductor: namely; Antimony Sulfide, or Sb_2S_3. The ZnO layer will be constructed of nanowires, and we will investigate the effect of changing the wire concentration, shape, length, and thickness. Both the inorganic n-type semiconductor, Sb_2S_3, as well as the p-type semiconductor, CuCSN, will be altered by tuning the morphology, ratio of the p and n-type layers, and thickness. Fatigue and bending tests will be applied to each cell, to observe the effect of modifications to the structures flexibility. Traditional efficiency tests will also be applied before and after bending, but not during due to difficulties calculating area and applying bending during testing. Lastly given appropriate time and sufficient testing of the individual cells, mechanical design ideas will be applied to the structure of the solar panel to investigate covering larger areas while still maintaining flexibility and good efficiency.

3. Background

In order to design the best possible flexible solar cell, the basic working principles of the cell must first be understood. The methods of light absorption, charge separation, and charge transfer must be determined to be able to take advantage of all the aspects needed to increase efficiency and flexibility. Beyond these basic working principles, the various state of the art flexible panels must be investigated. The methods being used by others in the field will give insight into options that work well, and ones that do not, and ones that have been explored thoroughly. This research will help guide the direction of this project going forward.

3.1 Working Principles of a Solar Cell

All types of solar panels follow a basic layout that consists of a series of layers that work together to allow electrons to flow through a functional circuit. The cathode is the conductor closest to the side of the p-type semiconductor layer, and is usually made from a metal in a grid like pattern, although our cathode is a solid metal film of Au/Pd. Below this layer lies the two semiconductor layers. The semiconductors are typically separated into two layers, called n and p type semiconductors, n standing for negative and p for positive. Usually to obtain the two layers of a semiconductor the material will need to be doped. There are also materials that act as intrinsic n or p type semiconductors that do not need to be doped. Doping introduces a small amount of an alternate element into the main semiconductor material. To make the n type layer of the semiconductor the element that is introduced into the main structure has more valence electrons to create free electrons and the p type semiconductor layer has less valence electrons, in order to create vacancies ("holes") for the free electrons to occupy. These are the layers where the charge is separated and transported. These layers can consist of a variety of materials which differ in many of the major types of solar cells that exist today. A common example is crystalline silicon in which one layer is doped to promote charge movement and the other layer is doped to become a charge receiver. The back-contact acts as the anode and finishes off the circuit. The anode layer of thin film solar cells is especially important in flexible solar cells, because it can often be the limiting flexible layer. Two of the primary options are Indium Tin Oxide (ITO) and Aluminum Doped Zinc Oxide (ZnO-Al).

3.2 State of the Art

Research to study the state of the art for solar cell technology was done by considering both technologies in industry and laboratory results. Industry results include more developed panel concepts and constructions, including silicon panels, while laboratory results feature new nanostructure

technologies and cell layers, that have only been recently developed or not widely implemented. These include nanostructures such as Carbon Nanotubes (CNT), Silver Nanowires (Ag NWs), Zinc Oxide (ZnO) nanowires, and cell layers TiO_2 and Sb_2S_3

3.3 Cell Types

Below we will discuss some of the various semiconductors in use in the field.

3.3.1 Crystalline Silicon Cells

Crystalline silicon cells make up 90% of the solar panels that exist in the world today. Within the distinction of crystalline cells there are two types, which are monocrystalline and polycrystalline. Monocrystalline cells are formed into a single crystal from ingots and have efficiencies ranging from 15%-20%, while polycrystalline panels are simpler to manufacture they also have low efficiencies, ranging from 13%-16%. On top of being more efficient, monocrystalline panels are also more space efficient, longer lasting when compared with other types of cells, and more efficient in higher temperatures. The last type of silicon cell is amorphous, which while being the least common silicon panel type, is most suitable for thin filmed flexible panels. These types of cells are formed from using vapor deposition to create a thin layer of silicon on a substrate made of metal, glass, or plastic. The thickness of these cells is roughly 1/300 the size of a monocrystalline silicon cells. The efficiency is around 7% due to the difference in structure of the silicon.[1]

3.3.2 Copper Indium Gallium Selenide (CIGS) Cells

Copper Indium Gallium Selenide (CIGS) is one of the many options being explored in the field of flexible cells. The CIGS layer acts as the p-type semiconductor in the panel, where it's supreme photon absorption coefficient helps to trap as much energy as possible, and is coupled with Cadmium Sulfide (CdS) as the n-type semiconductor.[2] Besides its good absorption properties, what makes CIGS so good for flexible solar panels is how thin it can be layered. This ability to make the semiconductor only 2-4 µm thick allows the panels to be super flexible, when printed on a flexible material. MiaSolé, a company specializing in CIGS panels, prints their panels on a thin stainless steel back sheet. This allows the panels to be very flexible in all directions, however, there is still the possibility of putting a crease in the stainless-steel sheet if bent too far. MiaSolé's panels are some of the most efficient on the market currently though, achieving almost 17% efficiency.[3]

[1] ("Amorphous Silicon Solar Panels," 2013)
[2] (Stanbery, 2002)
[3] ("MiaSolé Product Page," 2016)

The work being done in laboratories to improve CIGS efficiency has led to some very impressive results in recent years. As of June 15th, 2016, the world record for CIGS efficiency was set at 22.6%, by the Center for Solar Energy and Hydrogen Research Baden- Württemberg (ZSW). This was achieved on a 0.5 cm^2 test cell deposited on glass, so while this result would not be translatable to a full scale flexible panel, it shows promise for full scale panels in the future. ZSW used co-evaporation to deposit the CIGS layer, and increased the efficiency by both improving manufacturing techniques and by performing a post-deposition treatment of the CIGS surface with alkaline metal compounds. The researchers at ZSW believe their advances could lead to 18% or higher efficient panels, at a cost of 25 cents per watt.[4] At this price point, thin film panels can start to become a viable option for public use and potentially rival Silicon based panels.

Another key material in CIGS panels is the Cadmium Sulfide (CdS) n-type semiconductor. CdS acts as a buffer layer in the p-n heterojunction layer, preventing the panel from short circuiting. The key with CdS is to get the film into a stable, hexagonal structure. This can be a problem, as some deposition methods, like Chemical Bath Deposition (CBD), tend to deposit the CdS as a cubic structure. CBD is one of the leading methods for deposition though, since this method produces stable, adherent and hard CdS films; CBD is also a very simple method of deposition. To achieve a hexagonal structure post deposition, Choubey et al. proposed annealing the CdS layer, in order to change the structure. Annealing the film ended up improving all the properties of the CdS film, as transmittance increased, the band gap decreased due to the decay of hydroxides, and the conduction increased due to sulfur vacancies.[5]

While CIGS panels may represent one of the best options in terms of flexible solar panels, they are a subject that has been covered extensively, and have been relatively mastered. The deposition of the CIGS layer can also be highly toxic, as Hydrogen Selenide (H_2Se) is often used as the source for Se.[6] These factors make exploring CIGS panels a non-option for this study, as there is plenty of work already being done, and the toxicity poses challenges for the equipment available.

3.3.3 Cadmium Telluride (CdTe) Cells

Cadmium Tellurium cells are the second most common solar cells after silicon cells. These cells are relatively easy to manufacture and have lower costs than silicon solar cells. The efficiency of these cells can reach over 22% and in commercial applications have been reported at over 16% efficiency.

[4] (Brusdeylins, 2016)
[5] (Choubey, Desai, Kale, & Kumar, 2016)
[6] (Stanbery, 2002)

Most cells are produced as a single p-n heterojunction structure with a p-type CdTe layer and most often an n-type layer of cadmium sulfide (CdS). These materials are direct-band gap materials, with a band gap energy of close to 1.45 eV, which allows for high absorption rates because the band gap energy is well matched with the solar spectrum. CdTe cells can be produced via thin film deposition thus allowing for a more flexible solar cell. Construction of CdTe cells is typically completed by adding a TCO and a copper back contact. Although the copper back contact is frequently added Cu atoms can diffuse into the semiconductor and accumulate in the p/n junction, creating defects within the cell layering.

The highest efficiencies of CdTe Cells have been reached through Cadmium Chloride ($CdCl_2$) vapor treatment. This process takes place before the back contact is added on and in an oxygen-rich environment at temperatures well above 300 °C. Although this vapor treatment has led to much greater efficiencies, for flexible applications of this panel type annealing at temperatures above 100°C would lead to ruining the substrate, and nixing the efficiency of the cell.[7]

3.3.4 Perovskite Cells

Beginning in 2009, methylammonium lead halide perovskites were synthesized and after testing, were found to have good absorber qualities for use in solar cells. Perovskite was initially heralded as an attractive option because of the ease with which it could be prepared and processed. Originally used as a sensitizer in dye-sensitized cells, an efficiency of only 3.8% was obtained. The reason for the efficiency being low in these tests were because some of the perovskite would form solids within the electrolyte.[8]

Perovskite solar cells have an average efficiency of 7% under laboratory conditions. In some cases, certain solar cells have reached efficiencies of over 20%. They can be made with PET conductive substrates to complete the inner circuit of the cell. All manufacturing processes except for the annealing of buffer layers, manufacturing can be done with a roll to roll process as well. The manufacturing of these cells is relatively easy compared to some other types of cell. The perovskite material is also flexible; the cell declines only 0.1% after fifty bending cycles.[9] Despite the obvious benefits to this cell type there are still safety issues due to the cells lead content and questions of its stability in actual

[7] ("Cadmium Telluride," 2016)
[8] (Malinkiewicz et al., 2014)
[9] (Roldán-Carmona et al., 2014)

devices. With stability as a major concern, applying this type of cell for mechanically flexible applications could lead to durability issues and drastically lower efficiencies after bending.[10]

3.3.5 Dye-sensitized Solar Cells (DSSC)

Dye-sensitized solar cells are another type of cell where the tasks of light absorption and charge carrying are separated unlike other types of cells. In these cells light is absorbed by a sensitizer which touches the semiconductor layer of the cell, this is typically TiO_2. Charge separation occurs when the photons reach the semiconductor layers via the dye layer. These dyes are synthesized to absorb light across a broader spectrum compared to other types of solar cells.[11]

DSSCs can be categorized into two different types, liquid and solid-state, with the difference coming in the phase of the electrolyte. The most typical configuration for a liquid electrolyte DSSC is glass/FTO/TiO2/dye/liquid electrolyte/platinum and the most typical configuration for a solid electrolyte DSSC is glass/FTO/TiO2/dye/solid electrolyte/cathode. The performance of these cells tended to differ greatly with solid-state DSSCs achieving up to 8.5% PCE and their liquid counterparts achieving a much more substantial 12% efficiency.[12] This was until recently when perovskite solar cells, a type of solid-state DSSC, reached efficiencies of 15%. The main reason that the solid-state cells had lagged behind liquid cells in efficiency was because the Hole Transport Material (HTM)/dye reactions were less ideal than the iodine/iodide-redox couple that occurred in the liquid cell. Since HTM's are solid, pore filling of the material with the dye has also been deficient. This deficiency creates incomplete dye regeneration, leading to a much less stable cell. Solid-state cells also have high recombination rates within the active layer and a lower hole mobility. These drawbacks have been mostly alleviated as dyes with higher absorption coefficients were introduced, HTM layers were made thinner, and process requirements to better fill the pores with the solid electrolyte were created.[13]

Even with the superior characteristics of liquid electrolytes, high hole mobility and low recombination, they are still limited by the low stability of the dyes. Because the electrolyte is so aggressive, it is not possible to use metal contacts for current collection in DSSCs. Without the ability to add silver fingers or a contact of any kind, the sheet resistance after scaling above 1 cm^2 resulted in reduced efficiencies. DSSCs stability when conditions such as stress, high temperatures (80°C), and light

[10] (Li et al., 2016)
[11] (Grätzel, 2011)
[12] (Heo et al., 2013)
[13] (Junghänel, 2007)

soaking are all applied is low when tested against the standards for thin film and crystalline silicon cells.[14]

3.3.6 Bi_2S_3 Solar Cells

Bi_2S_3 nanocrystals act as the n type semiconductor in thin filmed cells. The efficiency of these cells are roughly one percent making them less than ideal, but this cell type is being researched and improved constantly. These nanocrystals are relatively easy to manufacture, when compared to the single crystal solar cells that exist today. These cells can be produced via solution processing so that the thin film may act as the electron acceptor in the solar cell.[15]

One of the reasons that Bi_2S_3 is gaining attention in solar, is due to its relatively large band gap. Depending on the structure and processing of Bi_2S_3, the band gap can be up to about 1.8 eV. The band gap gets lower as the Bi_2S_3 layer gets thicker, and is lower if Bi_2S_3 is in its crystalline form. It was observed that the band gap decreased from 1.8 eV for a 50-nm thick, amorphous layer to 1.5 eV for a 200-nm thick, semi-crystalline layer.[16] This larger band gap at a thinner, amorphous stage could be promising for flexible applications, as the thinner profile will help with flexibility. Additionally, not needing to anneal the cell is important as high temperature processing methods could cause damage to any flexible substrate or other thin layer that is being used.

Some work has been done recently on Bi_2S_3 solar cells by D. B. Salunkhe et al., where TiO_2/ Bi_2S_3 thin film panels were created using Successive Ionic Layer Absorption and Reaction (SILAR). These cells were created by first layering TiO_2 onto Fluorine Tin Oxide (FTO) sheets, and then depositing Bi_2S_3 nanoparticles onto the TiO_2 using the SILAR method; a polysulphide electrolyte and a platinum coated FTO sheet finished off the cell structure. SEM images indicated that there was complete coverage of the TiO_2 by the Bi_2S_3, indicating that there should be optimal ohmic contact. The coverage improved as more SILAR cycles were performed, and efficiency increased as well. The best efficiency achieved, after undergoing 25 cycles, was only 0.148%. This low efficiency was attributed to either poor charge transport between the TiO_2 and Bi_2S_3 layers, or to the non-suitability of the polysulfide electrolyte that was used.[17]

[14] (Junghänel, 2007)
[15] (Rath, Bernechea, Martinez, & Konstantatos, 2011)
[16] (Pineda, Nicho, Nair, & Hu, 2012)
[17] (Salunkhe, Dubal, Sali, & Sankapal, 2015)

3.3.7 Bulk Heterojunction Solar Cells (BHJ)

P3HT:PCBM solar cells are a type of bulk heterojunction cell where there is no separation between the n and p-type layers of the semiconductor. Rather the n and p layers of the cell are a random mix of the two semiconductors, with more of the n type material at the top of the semiconductor and more of the p type material at the bottom. The full names of P3HT and PCBM are poly-3-hexylthiophene and [6,6]-phenyl C_{61} butyric acid methyl ester, respectively. Per one study in France, a weight ratio of 1:1 of the polymers yielded the best efficiencies in the cells. These cells are made on an ITO substrate and the substrate is spin coated with 50 nm of poly(3,4-ethylenedioxythiophene)-poly(styrenesulfonate) (PEDOT:PSS). Then the active layer of P3HT:PCBM is deposited by spin-casting from n anhydrous chlorobenzene solution and then the cathode is deposited on. From there the cells go through thermal annealing at 100°C.[18]

Crystallinity is an important factor that dictates the optical absorption of the P3HT nanodomains, this is shown when the cell is annealed properly as the efficiency of the solar cell is greatly increased.[19] To add to this, there are many other factors that can affect the efficiency of these cells, including structure and ratio of P3HT to PCBM.

The efficiency of this organic solar cell highly depends on the 3D morphology of the P and N layers that create the charge separation. The ideal layout for a solar cell with P3HT and PCBM is to create a fingered morphology shown in Figure 2b, whereas Figure 2c is a more realistic result. However, since these cells are just nanometers in thickness, it is difficult to create the desired effect. With electron tomography, the blend morphology and crystallinity can be studied to create more efficient cells.[20]

[18] (De Bettignies, Leroy, Firon, & Sentein, 2006)
[19] (Erb et al., 2005)
[20] (van Bavel, Bärenklau, de With, Hoppe, & Loos, 2010)

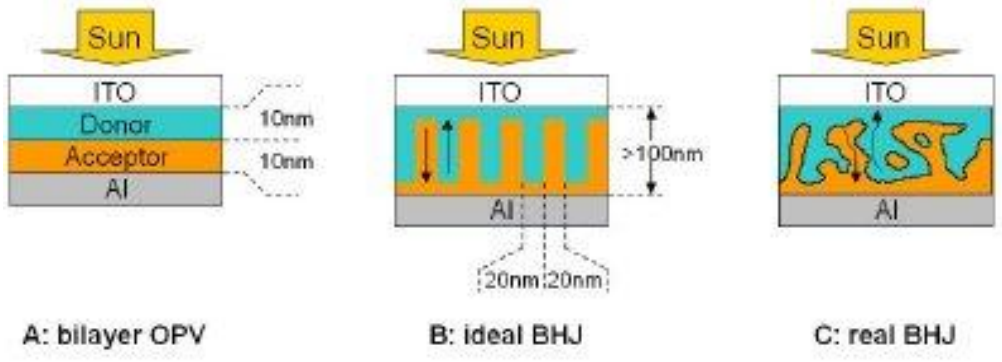

Figure 2 Organic Photovoltaic Solar Cell Structures[21]

Drawbacks of this type of solar cell includes limited efficiency and poor stability over lifetime use. Until as recently as 2016 the highest efficiency of these organic BHJ cells were below 10%, which is the threshold for what many think this type of cell must beat to be adapted to wide-spread applications. Currently the highest verified efficiency, which was on a 1 cm^2 cell, is 11% which although it has broken the 10% efficiency barrier this cell type still suffers from poor stability.[22]

The instability of this cell type can stem from issues that are both intrinsic and extrinsic. The intrinsic factors include factors within the cell, such as reactions within the active layers of the cell and between the active area/electrode interfaces, while extrinsic factors are issues that arise from environmental factors outside the cell. The table below shows the responses to different mechanisms that can cause the cell to fail.

Table 1 Root Cause of Failure in Solar Cells[23]

Stress	Response
Mechanical	Delamination, electrode failure, packaging failure
Temperature	Acceleration, delamination, morphological changes, diffusion
Light: special response, total intensity	Photochemical oxidation, photobleaching, yellowing, mechanical failure
Oxygen: humidity, water	Donor/acceptor oxidation, electrode oxidation, charge extraction, charge in mobility, TCO etching, interface failure
Coupled effects: water and mechanical, light and mechanical	Interconnect failures (in addition to above mentioned failures)
Electrical: electric field, columbic charge	Localized heating, shorts

[21] (Haeussler, 2009)
[22] (Scharber, 2016)
[23] (Brabec et al., 2010)

3.4 Charge Collector Layers

Some of the materials that are being used as charge collector layers in solar cells.

3.4.1 Transparent Conductive Oxides (TCOs)

Paramount to the success of any solar cell is the ability of its anode and cathode layers to create a current so that electricity can be produced. In thin film technologies, including solar cells, Transparent Conductive Oxides (TCOs) are most commonly used as the anode and cathode layers. What TCOs offer that make them desirable in thin film technologies are their flexibility and mix of good conductive and transparent properties. It most instances the conductive and transparent properties can also be adjusted. In our research on cell flexibility the layer in organic solar cells that was the most rigid was the anode layer. If one layer of the cell is less flexible it limits the overall ability of the cell to bend and flex to the desired degree. TCOs include common options like ITO, PEDOT: PSS, and ZnO along with other less common options such as Carbon Nanotubes (CNTs) and nanowires.

3.4.2 ITO and Possible Substitutes

ITO (Indium Tin Oxide) is a brittle, translucent material that is used in many solar cells produced today. Although ITO is the most commonly used anode layer it is not without its drawbacks or competition for replacing it. The three main drawbacks of ITO, as they relate to applications in Photovoltaic Solar Cells, are its previously mentioned brittleness, preparation, and high overall cost.[24] ITO is known to be quite brittle, so in solar cell application where flexibility is paramount, it may often not be the best choice and can limit overall device flexibility.[25] Although a rather flexible substrate with ITO can be fabricated if the ITO layer is very thin. Preparation is also an issue, in that, during fabrication temperature of greater than 200°C are needed, which for use on flexible substrates may be above the material glass transition temperature. The high temperature fabrication also adds to the high overall cost of ITO along with rising costs of indium due to limited resources. Materials that could serve as a replacement to ITO include PEDOT:PSS, carbon nanotubes (CNTs), graphene, and oxide-metal-oxide (OMO) multilayers.

3.4.3 Graphene

Another option as a charge collector that is still only be tested in labs, is graphene electrode sheets. These graphene sheets have properties that are very similar, if not better than, ITO. One

[24] (Minami, 2008)
[25] (Zhang et al., 2013)

drawback is that a uniform coating of the cells hole transporting layer with graphene can be hard to produce unless the graphene is doped with $AuCl_3$. Although this can be difficult to produce it does increase the conductivity and overall performance of the cell.[26]

3.4.4 Carbon Nanotubes (CNTs)

Carbon Nanotubes have begun to take on a larger roll in transparent electronics. CNT-based transparent conducting films are being developed as a substitute for TCOs in thin film solar cells, mainly ITO. Some of the advantages that CNTs have over ITO are its flexibility, cost, and manufacturability. A few of the main drawbacks of CNTs are its high resistivity, compared to equally transparent ITO. While a higher surface resistivity as some applications, for use in solar a greater resistivity only leads to a less efficient cell.[27]

To tailor CNTs to use in thin film solar cells doping methods have been used. What the doping of CNTs needs to accomplish to be more useful are to lower their electrical resistance and raise their conductivity. Doping does this by generating more free charge carries, through the free electrons created in n-type doping and vacancies created in the structure in p-type doping. There are drawbacks in the typical doping methods for CNTs. Doping using oxygen absorption can produce too many defects because it is difficult to control and ultimately reduce the conductivity. Also, doping alkali metals and halogens can produce tubes that are unstable in air, while the properties can remain good. One method of doping that has produced good results is doping with thermally-activated molybdenum oxides (MoOx). The results are stable and have optical to conductivity ratios up to 2.3, with the main drawback being that the annealing process takes place at 450°C.[28]

3.5 Nanowires

In this section, we will talk about the various nanowire layers that can be employed in solar cells.

3.5.1 Nanowires-Mat Electrodes

There are many options when it comes to the layout of solar cells, wherein flexibility and efficiency are leveraged against each other. One of the methods used to enhance flexibility is the use of nanowires as the electrode. The thinness of these nanowires reduces the thickness of the panels and the mesh construction adds to the flexibility. These nanowires can be made from any conductive material,

[26] (Hyesung Park and Jill, 2010)
[27] (Dume, 2012)
[28] (De Volder, Tawfick, Baughman, & Hart, 2013)

normally being either copper, silver, or gold. At the University of North Carolina, Chapel Hill, a team worked on making solar cells using solar silver nanowires. [29] At the University of Michigan, another team worked on using copper for the nanowires.[30] Both teams managed to achieve quite flexible cells, but recorded less than ideal efficiencies.

3.5.2 Ag Nanowires

A cell with a silver nanowire matrix as the anode is in development at University of North Carolina. The other layers of this cell were as follows PEDOT:PSS, P3HT:PCBM, Ca, and finally an Al back contact, all layered on PET. The process started with layering the silver nanowires on the PET by spurting an aqueous solution of nanowires on the substrate, and then pressing the solution to adhere the nanowires. The PEDOT:PSS layers and P3HT:PCBM layers were spun cast onto the substrate, and then pressed on to the Al/Ca layer. The finished panel was then annealed at 150°C. This process worked well on a glass substrate, however, this annealing process was not viable for the PET substrate. The glass transition temperature of PET is 75°C, much below the annealing temperature. During this step, the PET layer deformed, and very likely allowed the silver nanowires to break through and short circuit. This lead the team to explore replacement options for the P3HT polymer, looking for options that could be annealed at lower temperature to facilitate the use of PET. PBnDT-FTAZ and PBnDT-DTffBT were both chosen as replacement options for P3HT. The team managed an efficiency of 2.5% for PBnDT-DTffBT, and the PBnDT-FTAZ achieved an efficiency of 1.4%. PBnDT-DTffBT shows great promise for flexibility, as it still achieved 90% efficiency even after being bent 120° (7.2 mm bend radius). While the flexibility of these panels is very good, there is still room for improvement in the efficiency. The team attributed the low efficiency to the low work function of the Ag nanowires/PEDOT:PSS and the poor ohmic contact between the Ag nanowires and the active layers.[31]

There has also been research and testing in cells that keep ITO as the anode layer, yet alter it to increase its flexibility and reduce its well-known high brittleness. A material that has been shown to exhibit the desired features when integrated with ITO are silver nanowires (Ag NW). Ag NW are an ideal fit to alter the traditional ITO layer because of their superior flexibility and resistivity and specular transmittance values which are comparable to ITO, as seen in Table 1 below.

[29] (Chen et al., 2013)
[30] (Yang et al., 2011)
[31] (Chen et al., 2013)

Table 2 ITO vs. Ag Nanowires Transmittance Comparison

Material	Sheet Resistivity	Specular Transmittance (Visible Region)
ITO	1-7x10^{-4} Ω-cm	80-83%
Ag Nanowires	1.67x10^{-5} Ω-cm	80-85%

The reason for the large range of sheet resistivity in ITO is that the lower range is crystalline ITO films and upper range is amorphous ITO films. Both are included because while crystalline ITO is used in non-flexible applications, amorphous ITO is what is primarily used in flexible organic solar cell (FOSC) applications because of processing temperature limits of the most used flexible substrates. The Ag NWs and ITO layer were fabricated using sputtering and simple brush painting techniques. The whole process can be reduced to three steps: the bottom ITO layer was sputtered onto the substrate, the Ag NW were then brushed onto the ITO, and finally the top ITO layer was sputtered using the under the same conditions as the bottom layer. This process is both simple and reproducible, giving it an advantage over CNT and graphene anode layers which are notoriously difficult to adhere to substrates. The results for this altered anode layer vs the normal amorphous ITO anode, included much improved flexibility and even improved efficiency (2.574% vs 2.282%). Although these efficiencies were low, the increased efficiency with the Ag NWs added in shows that it is not only viable but quite possibly outright better than the traditional ITO layer.[32]

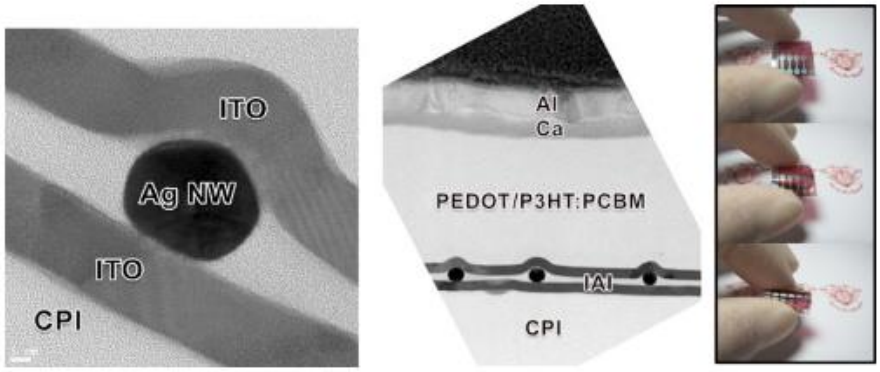

Figure 3 FOSC with Ag NW in anode

The above figure shows how the Ag NWs would fit interstitially in the anode layer and the cell. The reason for including this and why our right up for this one idea is so large, is that it looks like one of our initial ideas to create a more flexible anode layer. That idea was to create smooth bumps in the ITO

[32] (Choi, Kim, Noh, Na, & Kim, 2013)

to simulate hinges so that it would, in theory, be easier to bend. At first, we didn't know how to create those bumps, but Ag NWs serve as a great potential way to do that, while also creating a more flexible matrix with the top and bottom ITO layers.

3.5.3 Alternative Nanostructures

ZnO nanostructures have been studied in dye-sensitized solar cells (DSSCs) to increase light harvesting within the cells. The three types of nanostructures that were tested, were hedgehog-like hierarchical ZnO needle-clusters, three-dimensional (3-D) flowers and one-dimensional (1-D) ZnO nanowires. Of these three the hedgehog-like hierarchical needle-clusters showed the greatest light harvesting ability due to their high UV absorption, light scattering, and high surface area.

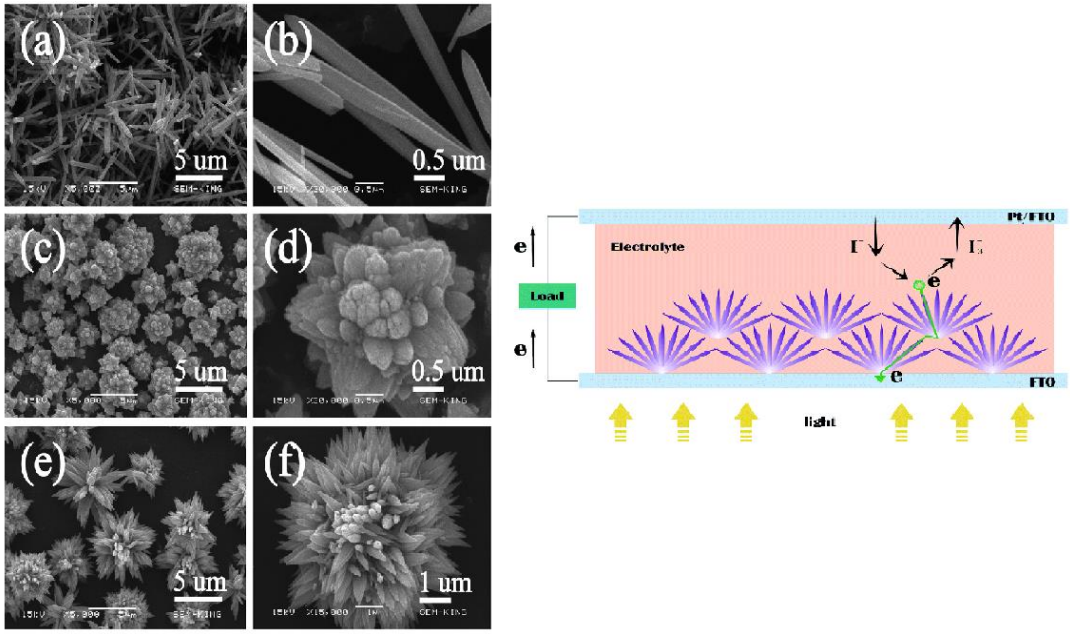

Figure 4 ZnO nanowire structure and application in DSSCs[33]

Although our project will not use DSSCs this research is applicable and backs up what we had originally thought the ZnO nanowires would add. By having the ZnO needle clusters penetrate the electrolyte layer of the DSSC, it reduced the charge transfer resistance. If the application of ZnO needle clusters can reduce the charge transfer resistance in DSSCs, then it should have the same effect if any semiconductor layer is formed on top of or in the same layer as the needle clusters.[34]

3.6 Processing Methods

Below we will cover some of the methods that are used to produce solar cells.

[33] (Qu et al., 2014)
[34] (Qu et al., 2014)

3.6.1 Roll to Roll Processing

One of the most prominent manufacturing methods for solar cells and flexible electronics in general is roll to roll (R2R) processing. R2R processing is a technique where a flexible substrate is moved through an assembly line where all the processes for the material to be manufactured into the needed application can be done. This technique is important because it can include both additive and subtractive manufacturing and can be done continuously. The order of manufacturing techniques for R2R processing vary with application, as R2R itself is not a specific technique, but rather an accumulation of techniques to process the product efficiently. Additional benefits of R2R is that it has a high throughput and a low cost to manufacture, making roll to roll an appealing choice for flexible solar cell production.[35]

3.6.2 Chemical Bath Deposition

Chemical bath deposition is a process in which semiconductor films are deposited on substrates in dilute solutions that will chemically form the ceramic based N semiconductor layer of the solar cell. Films including ZnS, Bi_2S_3, Sb_2S_3, n-CdS, and many others can be formed through this method. Growth curves can be studied to maximize optical and electrical properties of these materials. Chemical bath deposition is a slow process that is best suited for producing uniform films with a thickness ranging from 0.05-0.3 µm. The film thickness can be predicted up to a micron. The time for the deposition varies with each substance.

3.6.3 Vapor Deposition

Vapor deposition is the process that vaporized different materials to transport a material onto a substrate through evaporation. The material is vaporized in a controlled environment and then condensed onto a substrate. Vapor deposition can also lead to a chemical reaction through the process known as chemical vapor deposition. In many cases the reactants are kept in bubblers and temperature controlled baths to induce a reaction. The reactants are then bubbled in a certain flow rates to form the desired material on a certain substrate.[36]

3.6.4 Dip Coating

Dip coating is the manufacturing process in which substrates are submerged in a solution and then withdrawn at a controlled speed. The speed of withdrawal controls the thickness of the applied material, as show in Figure 4, where x_s is the final thickness, v is velocity during withdrawal, and C_1 and

[35] ("Roll to Roll (R2R) Processing Technology Assessment," 2015)
[36] (Wenas, Yamada, Takahashi, Yoshino, & Konagai, 1991)

C_2 are constants that are material dependent. The viscosity and surface tension also must be considered and can be altered for ideal thickness with the changing of temperature and composition of the solution material.[37]

$$x_s = C_1 v^{-1} + C_2 v^{\frac{2}{3}}$$

Figure 4 Equation for film thickness via dip coating[38]

3.6.5 Spin Coating

Spin coating which has already been mentioned in several sections, is a method for depositing solar cell layers via rapid spinning. The desired material for the layer is dissolved in a solution and after spinning is dried. In general, the higher the speed at which the liquid is spun the thinner the layer, although the final film thickness also depends on the viscosity and concentration of solution and solvent. Advantages of spin coating are its relative ease of production, speed, and ability to create consistently uniform layers. Spin coating is prominent especially in thin film solar cells because you can easily tune the parameters of spin speed, spin time, and concentration to yield a layer of your desired thickness. It is also popular due to the lack of coupled variables in the process, as just changing the spin speed or duration can predictably alter the thickness of the layer.[39]

The thickness of the layer can be predicted using Figure 5 below, where h is thickness, μ is viscosity, t is spin duration, and ω is angular velocity.

$$h \sim \left(\frac{\mu}{t\omega^2}\right)^{\frac{1}{2}}$$

Figure 5 Equation for film thickness via spin coating[40]

3.6.6 Drop Casting

Drop casting is another method of depositing a thin layer. With drop casting the process is simple, you dissolve the desired layer material into a solution, which is then applied to the substrate. With applied heat or over time the excess solution is evaporated leaving a thin layer of material behind. The main advantages of drop casting are its aforementioned simplicity, and low cost, as no expensive machines or equipment is used. The main disadvantage of drop casting is that because it is so simple it is difficult to get the exact layer thickness that is desired. If not under ideal conditions, any change in

[37] (Nostell, Roos, & Karlsson, 1999)
[38] (Hwang, Shoji, Endo, & Daiguji, 2014)
[39] (Sahu, Parija, & Panigrahi, 2009)
[40] (University of Florida)

evaporation rate or concentration of material along the substrate can lead to variations in thickness. Another drawback is that if the solution is not dropped on the entire substrate, sections of the substrate can have whole sections of that layer missing.

3.6.7 Screen Printing

Screen printing is a method of thin film deposition where the material that is deposited is pushed across the substrate at a uniform height. The benefits to screen printing are similar to drop casting, in that no expensive equipment is required. It also has the added benefit of producing a more uniform layer than crop casting. A disadvantage is that to be implemented screen printing needs to be done with a paste, which cannot be produced with many materials and requires more effort to produce that a solution with the material.

3.7 Cell Design and Laboratory Research

Our group focused on Antimony III Sulfide thin filmed cells for the project after deciding that it is the most reasonable material to work with. The focus for this project is on the engineering of the material, including the morphology of the layers, the manufacturing of the cells, each layer's material selection process, and the material science to make the cells more efficient.

The layout of the final cell design consists of a PET substrate, a thin ITO electrode, a thin TiO_2 blocking layer, an Sb_2S_3 n-type active layer, a CUSCN p-type active layer, and a gold/palladium mixture as the final electrode.

3.7.1 TiO_2 Blocking Layer

A team working under the European FP7 program successfully utilized a thin layer of titanium dioxide as a blocking layer in Perovskite solar cells. The team found that thin films of the TiO_2 lead to power conversion efficiencies of up to 11.5%. The team spin coated thin layers of TiO_2 over mesoporous TiO_2 layers to form a successful blocking layer. The fact that the layers can be ultrathin opens the potential to test this material's flexibility in this state. The substance is deposited at a temperature of 120°C, limiting the potential for use on a flexible substrate like many common plastics.[41]

3.7.2 Sb_2S_3 Solar Cells

Antimony III Sulfide (Sb_2S_3) is a very promising material for light harvesting and capture within the solar cell. The band-gap (1.7-1.8 eV) is part of what makes it appealing for use in solar. This is achieved when Sb_2S_3 is in its crystal phase, called stibnite, which can be achieved by annealing at 300°C

[41] (Chandiran et al., 2014)

for 30 minutes. This annealing is important for cells where CBD is used, as the Sb_2S_3 will be amorphous upon deposition, and performs much better when crystalline. Cells prepared with this annealed Sb_2S_3, paired with CuSCN, a p-type inorganic material, produced a power efficiency of 3.4%. When paired with 2,20,7,70-tetrakis(N,N-di-pmethoxyphenylamine)-9,90-spirobi-fluorene (spiro-MeOTAD) instead, this efficiency rose to 5.2%. This shows some promise for Sb_2S_3 as a material, however, there is some concern for its use in a flexible panel. Not being able to fully anneal it may hurt the efficiency, and there hasn't been much work done on how Sb_2S_3 will interact with ZnO.[42]

Another study looked at the feasibility of making Sb_2S_3 solar panels that used metal oxides. Al_2O_3 and ZrO_2 were both used in separate test panels, where Sb_2S_3 was used along with TiO_2, P3HT, PEDOT:PSS, and silver. In these cases, the Al_2O_3 and Zr_2O_3 acted as the n-type scaffold for Sb_2S_3 to interact with. The work here showed that Sb_2S_3 could completely fill the pores of the Al_2O_3 and ZrO_2, helping to increase efficiency. These two panels were compared to a more conventional panel using TiO_2, and achieved very close results. The TiO_2 panel managed an efficiency of 3.24%, while the Al_2O_3 and ZrO_2 managed an efficiency of 2.48 and 2.64% respectively. The Al_2O_3 and ZrO_2 managed to have higher open circuit voltages than the TiO_2 panel did, achieving 0.674 and 0.712 volts, as opposed to 0.504 volts.[43] This shows that there may be promise for using Sb_2S_3 with ZnO, where a usable efficiency might be achievable.

Itzhaik et al. also looked at Sb_2S_3 cells with TiO_2, achieving a similar efficiency of 3.37%. Of note from this paper was the observance of surface oxidation of the Sb_2S_3 after annealing. The team noted that surface oxidation was occurring post-annealing, which lead to lowered performance.[44] By not annealing the cells, we may have avoided this oxidation, and could possibly observe a better efficiency than if we followed Itzhaik et al.'s procedure.

3.7.3 CuSCN

As for the p-type layer, CuSCN was the final selection. CuSCN has the correct band gap for a solar cell applications. However, Kumara et al is among one of many groups that has had problems with the deposition of the material on cells. A few different methods were tested by this group. One of the more promising methods was when they dissolved the CuSCN in n-propyl sulfide. An issue with this method is that not all the CuSCN dissolves and the solution requires centrifugation to remove the excess

[42] (Moon et al., 2010)
[43] (Englman, Terkieltaub, & Etgar, 2015)
[44] (Itzhaik, Niitsoo, Page, & Hodes, 2009)

solid. The study concludes by stating that CuSCN is a promising material to use if certain obstacles, such as a consistent method of depositing it, can be overcome.[45]

A group at the University of Washington found that when CuSCN was immersed in ethanol electrolytes with cyanine dyes quantum efficiency of up to 80%. A threshold oxidation potential for the dyes was found in order to produce the highest possible laboratory efficiencies. The results of the experiment once again suggest CuSCN as a promising candidate for the p-type layer in solar cells.[46]

3.7.4 Zinc Oxide (ZnO) Nanowires

The use of ZnO nanowires within solar cells is an idea that has not been explored too much. There has been some work done in examining the interactions between ZnO and chemicals used in creating other solar cell layers but not much has been reported in terms of actual cell architecture. A lot of the work that has been done are on the optical-electrical properties of ZnO wires, however, most of this work looked at uses in the display market. Using ZnO nanowires could help improve the efficiency of flexible solar cells, to make them a more viable option. One of the downsides to ZnO is its high annealing temperature, which makes using plastic substrates more difficult. Methods for annealing ZnO at lower temperatures are being investigated, so that they might be used in flexible applications.

One of the main problems with using ZnO is that it is most efficient when it is in the crystalline phase. This normally involves annealing, which is problematic for flexible solar cells, as they are normally built upon a plastic substrate. ZnO is normally annealed at ≥300°C, while the highest quality PET has a glass transition temperature of 150°C. A study was done by Jagadamma et al. to investigate other methods to increase the efficiency of the ZnO, without having to anneal it at 300°C. The team used a solution processed ZnO thin film, creating a fully amorphous ZnO layer, which performed equally or better than previous examples of crystalline or nanoparticle ZnO. This layer of a-ZnO was found to work best when the surface was smooth, not rippled. The optimal thickness for this layer was found to be between 15-35 nm thick. This adverse effect of ripples is contrasting to that of crystalline ZnO, where rippling tended to increase performance. The a-ZnO cells managed to achieve a 3.95% efficiency in the best case. These cells also proved to be quite stable, maintaining 90-95% of its efficiency after being stored for 13 months without any preparation.[47]

[45] (Kumara et al., 2001)
[46] (O'Regan & Schwartz, 1995)
[47] (Jagadamma et al., 2014)

Zinc Oxide nanowires can be electrospun to create a nanofiber networks that can lead to efficiencies ranging from 0.9 to 2.23%. These ZnO nanowires help optimize the active area for both energy absorption and exciton dissociation. This study was done considering both organic and inorganic photovoltaics.[48] Another method is to use textured ZnO seeds for vertical nanowire growth. This method grows ZnO nanowires on any substance using either a gas or solution phase approach. Both processes use the decomposition of zinc acetate at 350°C to provide nucleation for growth sites. The following characteristics were deemed ideal for polymer solar cells: diameters of 15 to 65 nm, lengths of 250-400 nm, and separation gaps of 5 to 45 nm. The seed diameter range is 5 to 20 nm with thicknesses of 3 to 5 nm.[49] Aqueous solution processing is one of the simplest methods for the fabrication of ZnO nanowires. Solutions of zinc nitrate and hexamethylenetetramine successfully grew zinc nanorods (nanowires) on a variety of substrates that included PET and Si wafers.[50] The following picture is an example of how solution grown nanowires are created with zinc nitrate hexahydrate, thiourea, ammonium chloride, and ammonia.

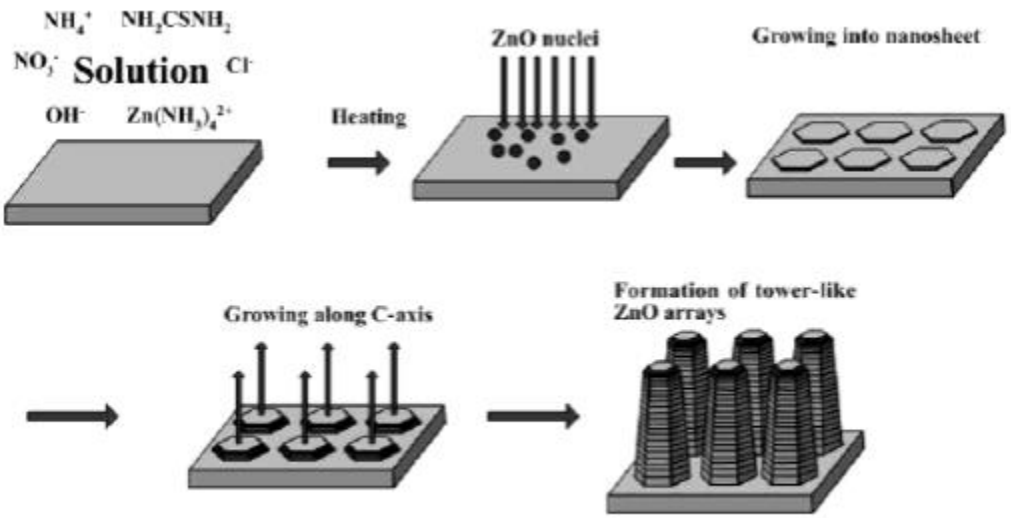

Figure 5 Growth of ZnO Nanowires[51]

[48] (Tanveer, Habib, & Khan, 2012)
[49] (Greene et al., 2005)
[50] (Z. Wang, Qian, Yin, & Zhu, 2004)
[51] (W.-W. Wang & Zhu, 2004)

Different Solution Methods for ZnO nanowires:

1: Zinc nitrate hexahydrate, thiourea, ammonium chloride, and ammonia

2: Decomposition of $Zn(OH)_4^{2-}$ in aqueous solution at 90°C in oil bath

3: Solution growth process using zinc nitrate and hexamethylenetetramine in aqueous solution

4. Decomposition of zinc acetate at 350°C

5. Zinc acetate and sodium dodecyl benzene sulfonate

ZnO has been looked at primary as a wide band gap semiconductor in diodes. It has also been researched and studied as a layer in BHJ organic solar cells. ZnO is prepared by dissolving Zinc acetate and sodium dodecyl benzene sulfonate in deionized water. The zinc acetate solution is slowly added to the sodium dodecyl benzene sulfonate solution while being stirred for 15 minutes. Next the samples are dried at 105 degrees C for approximately 4 hours and finally after being placed in a crucible are calcined at 950 degrees C for 6 hours.

3.7.5 ZnO Performance and Construction

Though ZnO has been research as a layer in these cell types, it was primary researched in its crystalline form, which is not flexible. Structures that are made of ZnO that have been recently fabricated are needles, nanorods, nanowires, tetrapods, nanocombs, nanopencils, nanotubes, and star-like. An application of interest to this project is growing ZnO structures on a ITO film/substrate base. Growing the ZnO directly on the structure would allow for varied designs to be created rather easily and if done correctly would create a flexible layer. The ZnO nanowires that were formed in the earlier described process were up to 500 µm in length, ranged from 5 to 20 µm in diameter, and generally stood straight up. When examining the optical properties of the ZnO microstructure that was formed two emission bands, one at the near band edge (370 nm) and another at the green emission (530 nm), were observed.[52]

3.7.6 Gold/Palladium

Gold and Palladium thin films are one of the many option available as a electric contact on the cell. One group at the Swiss Institute of Technology that studies dye-sensitized solar cells vacuum evaporated a transparent gold contact on top of the hole conducting layer. The group reported an incident photo-to-electron power conversion efficiency of 33% with their cell design. The group concluded that the use of dye-sensitized solar cells is a viable option for low cost solid-state solar cells.

[52] (Y. Wang, Tong, Xu, Özyilmaz, & Loh, 2011)

They can be flexible in part due to the thin electrode layer. In many cells, the electrodes are stiff metals that cannot bend.[53]

[53] (Bach et al., 1998)

4. Testing Methods

Once the cells have been manufactured, various tests will be conducted to determine flexibility, life time, and efficiency of the panel. While the main goal of this project is produce a flexible cell, achieving a moderate efficiency is also important. The testing methods for each of these factors will be outlined below.

4.1 Flexibility

The flexibility of the cell is important as a flexible cell is only good if it can be repeated and does not greatly affect the cell performance. To test flexibility, the final cell and each individual layer will be bent at a fixed radius. We will bend the cell for several cycles and use a Scanning Electron Microscope (SEM) to determine if any nano-level deformation has occurred. Electrical resistance of certain layers will also be compared before and after bending.

4.2 Efficiency

We will perform normal solar cell efficiency tests, observing efficiency at 1 sun and determining short circuit current and open circuit voltage. The efficiency will also be tested again after the panel has been bent to its ultimate radius, and again after it has undergone cyclic loading. In this way, we can see if flexing has any effect on long term efficiency, possibly indicating deformation as well. Comparing efficiencies between low temperature and high temperature annealed cells will also be done.

5. Methods

The different methods that we followed to create each layer in the cell are outlined within the sections below.

5.1 ITO/PET Substrate

The PET substrate was purchased from Sigma-Aldrich with an ITO layer already sputter coated on it. We purchased two different sheets, one with a surface resistivity of 60 Ω/square and another with resistivity of 200 Ω/square. We were curious to see what effect the different resistivity would have on cell performance. The ITO layer is 1300 Angstroms thick, and has been tested to maintain performance up to a 75-mm bend radius. The substrate was cut into rectangles with dimensions of 25 mm X 20 mm, as the diameter of the tube furnace limited cell width to 20 mm.

5.2 TiO_2 Blocking Layer

The TiO_2 layer was prepared in the method used at the Stevens Institute of Technology. We changed the annealing temperatures and times to make the method more suitable for our PET substrate. Two solutions were prepared for the samples. The first solution was .15 Molar of TiO_2 solution which is prepared by dissolving 0.055 mL of Titanium di(isopropoxide) (75% in propanol) in 1 mL of isopropyl alcohol. The second solution is a 0.30 molar TiO_2 which is prepared by dissolving 0.110 mL of Titanium di(isopropoxide) (75% in propanol) in 1 mL of isopropyl alcohol. Then, the sample was spun coat with the 0.15 Molar solution at 2000 rpm for 30 seconds, with tape covering half of the etched section of the cell and the ITO contact area for the full cell. The sample was then taken off the spin coater and the taped areas were wiped by a cotton swab with acetone. This was done to prevent any tape residue from burning on the contact areas. Then the sample was placed on a hot plate for 10 minutes at 80°C for the low temperature process done on plastic and for 5 minutes at 125°C for the high temperature process done on glass. The sample was then put back on the spin coater with the 0.30 molar solution for 30 seconds at 2000 rpm and again with the tape covering the same areas. Once again, the sample was heated for 10 minutes at 80°C for the low temperature process and 5 minutes at 125°C for the high temperature process. The final spin coating was with the 0.30 molar solution for the same specifications as previous and the sample was placed on the 80°C hot plate overnight for the low temperature process and 500°C for 15 to 30 minutes for the high temperature process.

5.3 ZnO Nanowires

For the ZnO nanowires, we focused on the method performed by Law et al. This method was chosen due to its low temperature construction. Other students in our lab had been using a Zinc Acetate

Dihydrate (ZAD) method to relative success, however, this method requires annealing at 350°C, and was thus ruled out. Our ZnO ink method was conducted as follows. A seed solution was made by mixing 5 mM of the ZnO ink solution in Isopropyl alcohol and sonicating the solution for 30 minutes. The seed solution is then spin coated on the samples for 40 seconds at 2,000 rpm, three times. Between each round of spin coating, the cell is rinsed in Isopropyl Alcohol and dried. While the spin coating is being done, the chemical bath for growing the nanowires is prepared. We chose a 50 mM concentration for our growth bath, to get the desired wire length and wire density. The bath is made of 2 mL of Poly(ethyleneimine) (PEI), 2.97 g of zinc hydride , 0.4 g of Hexamethylenetetramine (HMT), and 100 mL of DI water. This solution was stirred with a magnetic stirrer until thoroughly mixed and clear. The cells were then suspended in this solution, with the active side facing down at a slight angle, and solution was then heated to 90°C. The top of the beaker was covered in aluminum foil to ensure minimal heat loss. After 2 hours, the bath was swapped out for a fresh one. At the 4-hour mark, the cells were removed and washed with a mixture of equal parts IPA, Acetone, and DI water, then dried with air.[54]

5.4 Sb_2S_3 Thin Film

The Antimony Sulfide layer was produced using the cold bath method outlined by Nair et al. First, 0.6 g of Antimony Chloride (SbCl III) was mixed with 2 mL of Acetone. This solution was sonicated for 10 minutes, and then put in the fridge to cool. Next, 3.95 g of Sodium Thiocyanate ($Na_2S_2O_3$) was mixed with 25 mL of DI water, and stirred with the magnetic stirrer until thoroughly mixed. This solution was then also placed in the fridge to cool, along with 75 mL of DI water. After a few minutes, the three solutions were poured into a beaker inside the fridge; first, the SbCl (III), then the $Na_2S_2O_3$, and finally the DI water. This new solution was mixed by magnetic stirring in the fridge for 2 minute at the lowest speed. After two minutes, with the stirrer still spinning, the substrates were placed in the solution, vertically with the active side facing towards the center of the beaker. The cells were left in the solution for 6 hours, and then removed and rinsed with the IPA/Acetone/DI water mixture, then dried.[55]

There is another Sb_2S growth method that our group tried. This method involved a similar chemical reaction at 40 Celsius instead of the cold bath method. The results from this method were less promising than the cold bath so we switched back to the cold bath method after several attempts. This method could be studies more in depth to save time while creating these cells. Another possible method

[54] (Law, Greene, Johnson, Saykally, & Yang, 2005)
[55] (Nair, Pena, Campos, Garcia, & Nair, 1998)

is to spin coat Sb_2S onto the substrate itself and skip the chemical bath all together. However, our group was not able to get a hold of powdered Sb_2S for this process.

5.5 CuSCN Thin Film

Copper Thiocyanate (CuSCN) was then deposited using spin coating, as outlined in Yaacobi-Gross et al.'s paper. 0.15 g of CuSCN was mixed with 5 mL of diethyl sulfide, and spun with the magnetic stirrer for 15 minutes. This solution was then spun coat on the cells for 30 seconds at 800 rpm. After spin coating, the layer was annealed at 65°C for a few hours, mostly done to evaporate any leftover dipropyl sulfide.[56]

5.6 Au/Pd Back Contact

The back contact was created by sputter coating a layer of a Gold/Palladium (AuPd) mixture for 3 minutes. This created a 50-nm thick layer

[56] (Yaacobi-Gross et al., 2015)

6. Results

Below we will discuss the results of our two major tests, efficiency and flexibility. We will examine the efficiency tests of cells on both PET and glass substrates, along with the low and high temperature annealing results. For flexibility, we will examine the before and after SEM images of each layer in the cell, to examine their degree of flexibility.

6.1 Efficiency

We managed to produce a working solar cell during the course of this study. Unfortunately, the efficiency was quite low, with our best cell achieving an efficiency of roughly 0.0015%. Using the solar simulator (300 W Xenon Lamp, Newport), we could simulate the conditions of one full sun for testing. We used a potentiostat (Biologic SP-200) to measure both current generation and power generation in the cell.

6.1.1 FTO Glass with High Temperature Annealing

We managed to achieve a working cell on FTO glass with high temperature annealing of both the TiO_2 and Sb_2S_3 layers.

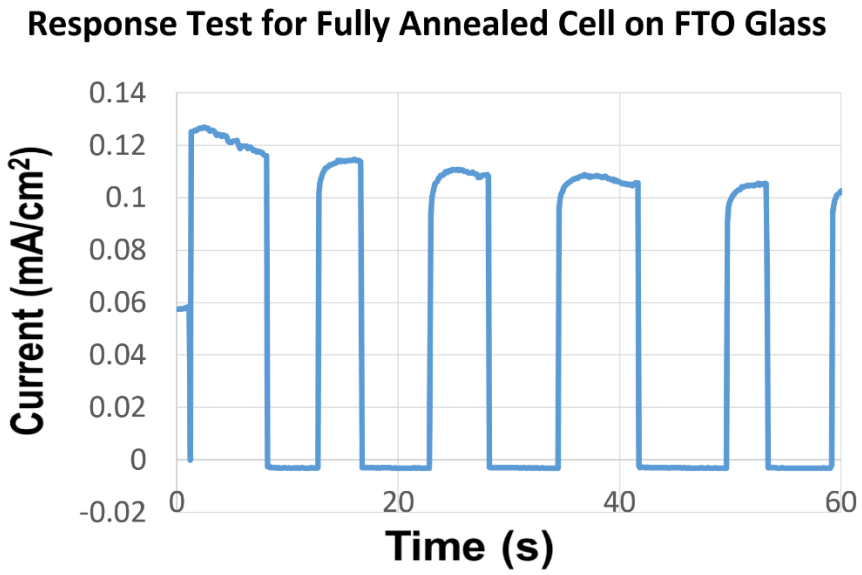

Figure 6 Light Response for Fully Annealed FTO Glass

The graph in Figure 6 shows that this cell did in fact respond to light. When exposed to light, the cell generated a short circuit current density (Jsc) of roughly 0.1 mA/cm^2. Once the light source was blocked, the current dropped back down to 0 mA/cm^2. This indicated we had a working solar cell, and gave us a short circuit current that could be used to dial in our measurements to graph the power curve.

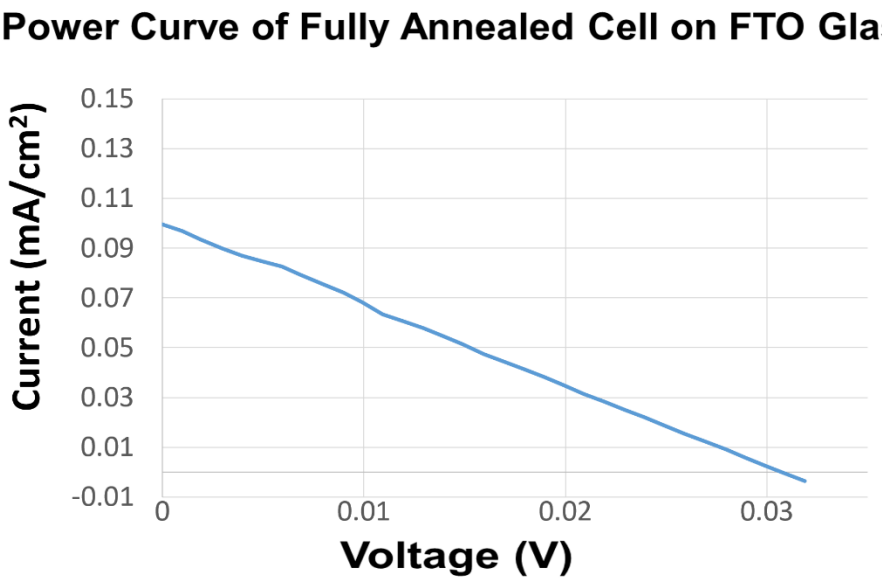

Figure 7 Power Curve Generated by FTO Glass, Fully Annealed Solar Cell

Once we knew roughly what the short circuit current would be, we tested the current-voltage curve, which showed us that the open circuit voltage (Voc) is 0.03 V. Using the area under this curve, we could calculate the efficiency of the cell. Approximating the curve as a triangle, we could use the equation $\frac{1}{2}J_{sc}V_{oc}$; then divide this value by the power generation from the solar simulator, roughly $100\frac{mW}{cm^2}$. This gave us our efficiency value of 0.0015%.

6.1.2 FTO Glass with Low Temperature Annealing

Our low temperature annealing attempt on FTO glass unfortunately did not produce a working cell. This cell was meant to act as a point of reference to the plastic cell, where we could compare the effects of annealing without having to worry about what effect flexibility might have on efficiency. One of the Au/Pd contact strips got pulled off by the copper tape during testing, leading to a poor contact. The other contact on the cell recorded a zero value during testing, indicating a short. Without a second point of reference, we couldn't be entirely sure if this short was due to the low temperature annealing or if we happened to have sputtered the gold on a particularly porous part of the cell.

6.1.3 ITO Plastic with Low Temperature Annealing

We noticed some interesting behavior with the ITO plastic cell during testing. During the light response test, the current appeared to drop when the light source was blocked. This would indicate a working cell; however, the current is so slight that it is difficult to differentiate from the noise of the potentiostat instrument.

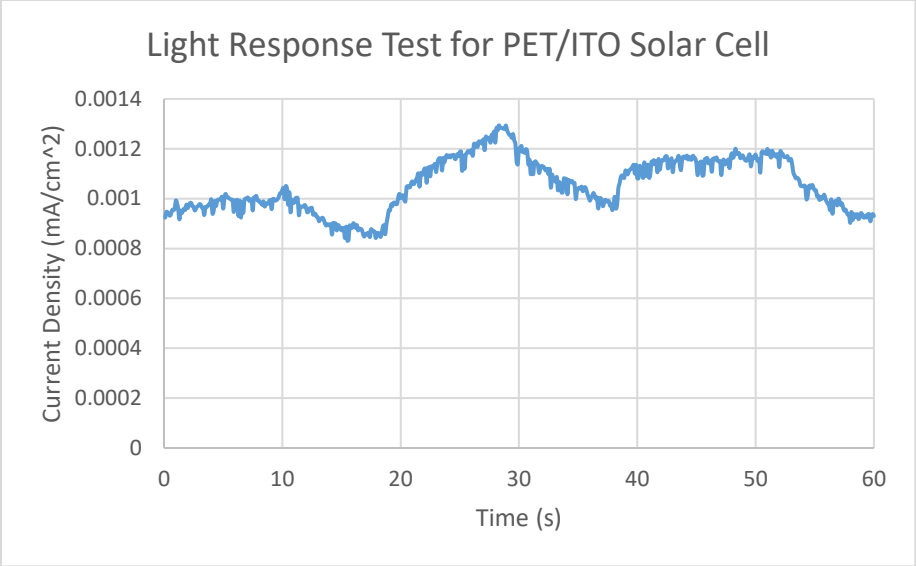

Figure 8 Light Response Before Bending for ITO Plastic Cell

The light response of the ITO plastic is much slighter than in the FTO glass sample mentioned above. When the light source is blocked, the current begins to gradually decline, rather than produce the sharp drop seen previously. Also, when the light is unblocked, the current begins to slowly rise, rather than jump back to the cell's short circuit current value. The current value also never seems to stabilize, peaking at a value of 0.00055 mA, but also registering at the 0.0004 mA and 0.0005 mA marks as well.

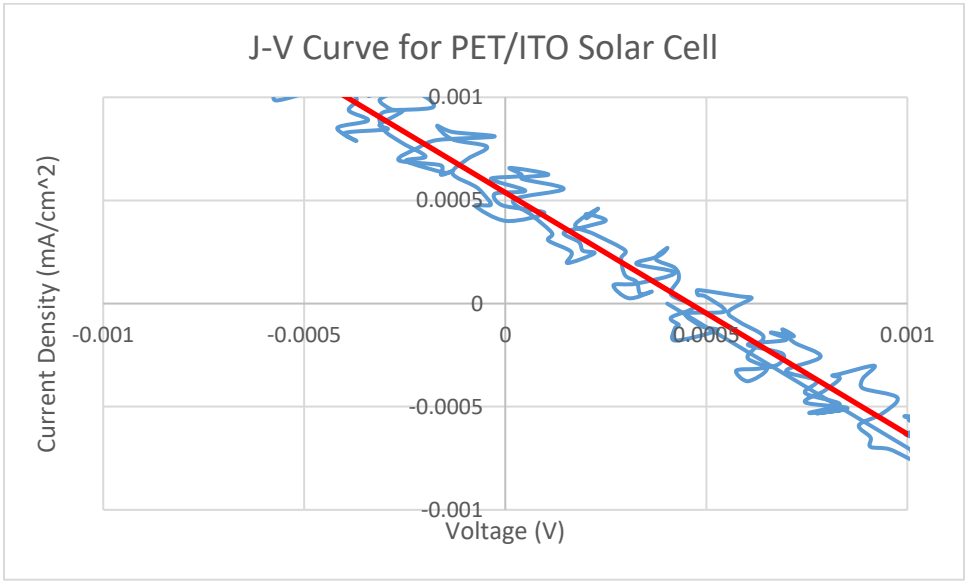

Figure 9 J-V Curve for ITO Plastic Cell Before Bending

We also graphed the power curve for this cell, anticipating it to be rather small. We did achieve a non-zero result, however it's so slight that it was hard to differentiate from the potentiostat noise. Looking at the trend line, we can say that the cell had a Jsc of roughly 0.0005 mA/cm^2, and a Voc of roughly 0.00048 V. Going forward creating a working cell on this substrate will be possible, but different methods may be needed to get around the low annealing temperatures.

6.1.3.1 ITO Plastic After Bending

Knowing that the ITO plastic cell worked to some small degree, we went ahead with bending it, to see how this would affect the efficiency of the cell. The cell was bent tip to tip 50 times with the copper contacts still attached, to preserve the surface of the cell as much as possible. It was then replaced and tested as it had been before.

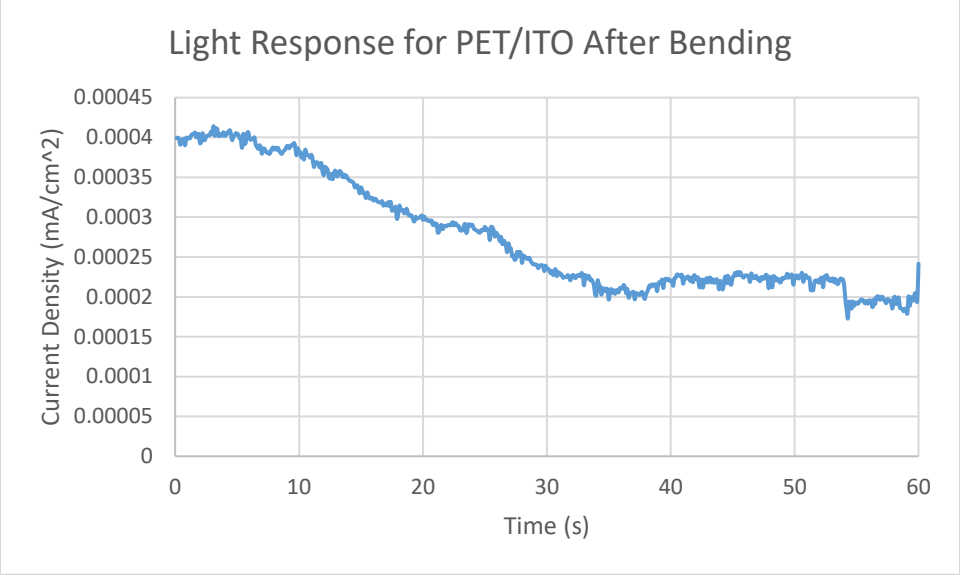

Figure 10 Light Response for Plastic Cell After Bending

Measuring the light response of this cell proved difficult. Over the course of about 6 tests, we got some varied results. The cell appeared to respond to light occasionally, but not consistently. The short circuit current value also appeared to have dropped from its previous value, making measuring even more difficult.

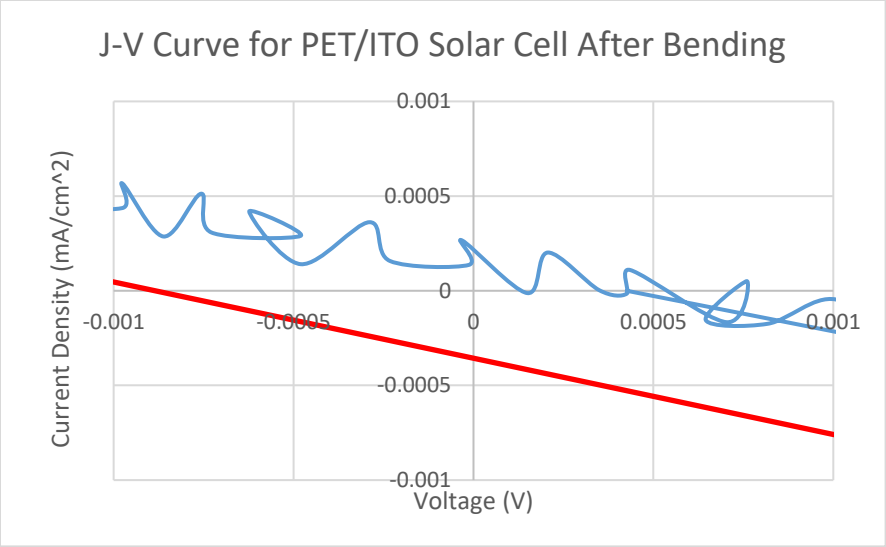

Figure 11 J-V Curve for Plastic Cell After Bending

We went on to measure the power curve, using the knowledge that the short circuit current would be quite small. We turned the resolution up as high as the device allowed during this test, which resulted in the irregular shape of the graph. Despite this, it appears that the curve does not go through zero. This means that the cell still works to some degree, but has certainly dropped off from where it was before bending.

While we've shown that it is possible to produce a working cell on the ITO plastic substrate, this test shows that the ability of the cell to flex and continue working is still in question. The small performance achieved quickly degraded after being bent, essentially destroying the cell.

6.1.4 Light Absorption of Sb_2S_3

While testing the efficiency of the cell, we also looked at what wavelengths of light the Sb_2S_3 layer was absorbing. Using the solar simulator, we first took a baseline reading of the light levels being emitted by the Newport machine. We then placed a cell, in this case the working FTO glass sample from above, in front of the meter. The cell was placed with the bare glass face towards the light source. We collected data from two points; between the two Au/Pd contacts, where there was just Sb_2S_3, and on the Au/Pd contacts, where this mixture could block more light.

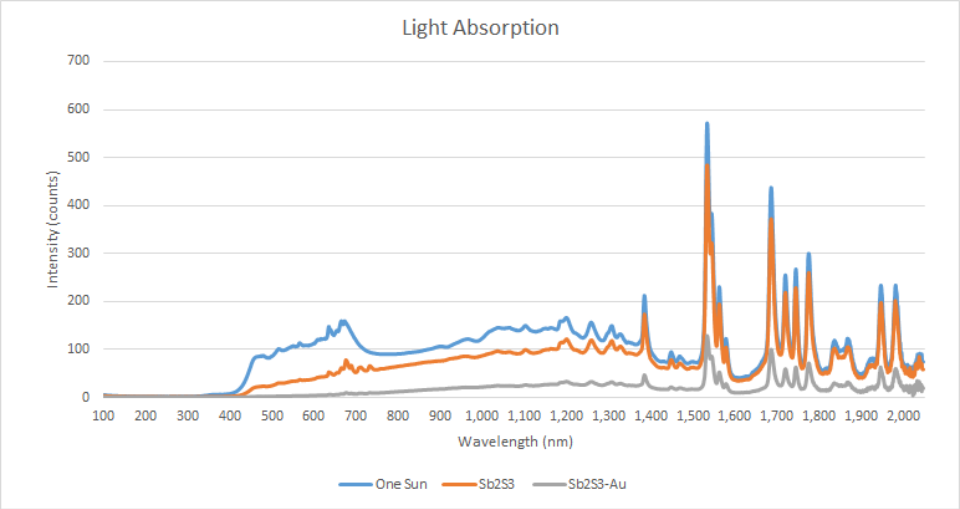

Figure 12 Wavelengths Absorbed by Sb_2S_3

Taking the data from the Figure 12, we can calculate the percent light absorbed by the Sb_2S_3. Looking at the amount of light absorbed will allow us to see if the Sb_2S_3 layer is the reason for our low photocurrent.

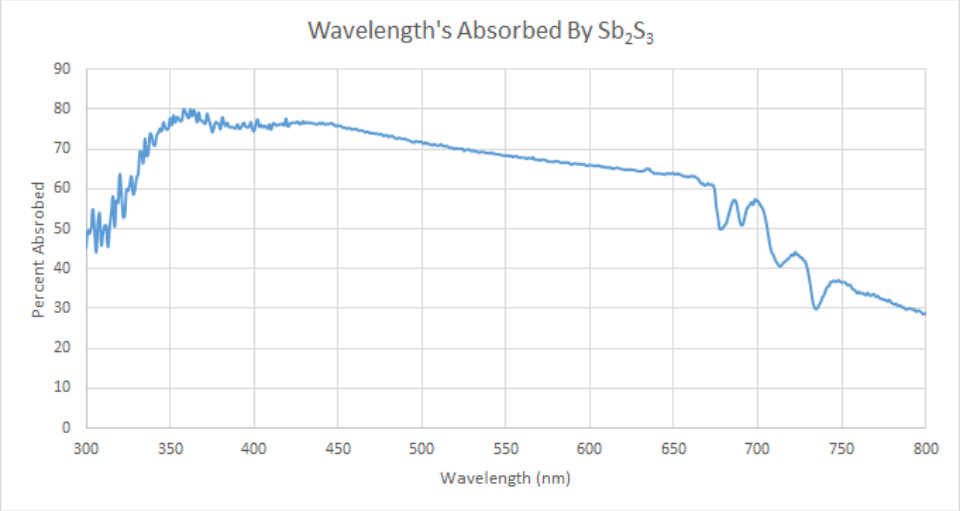

Figure 13 Percent of each Wavelength Absorbed by Sb_2S_3

Knowing that the band gap for Sb2S3 is in the 1.7-1.8 eV range, we can determine that Sb2S3 should be absorbing light in the 725-nm wavelength area. From this graph, we see that about 50% of the light is being absorbed at the 725-nm wavelength, which indicates that plenty of sunlight is reaching the Sb_2S_3. This should have been enough to produce a higher photocurrent, thus indicating that there is a problem elsewhere in the cell that is inhibiting the overall efficiency.

6.2 Flexibility of Layers

We examined each layer in the final cell design to ensure that they were indeed flexible, and that they did not crack during use. If any of the layers were to break during bending, this could have caused our cells not to work. To observe this, we created separate films on ITO/PET substrates, each having only one layer coated on it. We took an SEM image of the substrate, taking note of the SEM coordinates of the image. We then bent the substrate repeatedly by touching the ends of the substrate together, so that we had a consistent radius. After, we placed the substrates back on the SEM chuck in the same place they were originally, and went to the coordinates of the before picture. This way we would see the difference resulting from bending on the same area of the substrate.

All substrates were bent tip to tip, which gave us a consistent bend radius of about 4 mm. The ITO and Au/Pd cells were bent 50 and 100 times, while the other layers were just bent 50 times. We also calculated the strain induced in each layer due to bending, using the equation $\varepsilon = \frac{\tau}{2r}$. As we could not get a good side view of our cells to measure layer thickness, we used the stated layer thickness from each paper where the procedure was derived.

Table 3 Strain Induced during Bend Tests

Material	Stain Induced	Thickness of Layers (nm)
ITO	1.625×10^{-5}	130
TiO_2	1.25×10^{-5}	100
Sb_2S_3	2.5×10^{-6}	20
CuSCN	1.625×10^{-6}	13
Au/Pd	3.125×10^{-6}	50

These bending tests were important in understanding potential reasons why our flexible cell performance was poor, and how these materials might be used going forward.

6.2.1 ITO and Au/Pd Bending

The two conductive layers were tested both by measuring their resistivity before and after bending and by imaging. These two layers are the most important in terms of breaking. If the absorber layers crack, it's not quite as important, as the charge is being carried vertically to the layers below. The conductive layers need to transport charge horizontally to the contact leads. Any cracking in these layers could cut off the flow of electricity, thus reducing the amount of power that the cell produces.

Table 4 Change in Resistance Due to Bending

	Before Bending	After 50 Bends	After 100 Bends
ITO	190 Ω	1473 Ω	1640 Ω
Au/Pd	117 Ω	290 Ω	626 Ω

From these results, we could clearly see that ITO was not going to be serviceable at this bend radius. The sheet resistance increased 7.75 times after 50 bends, and was up to 8.6 times after 100. This increase in resistance would certainly hurt any efficiency that could be achieved on the cell, possibly ruining it all together.

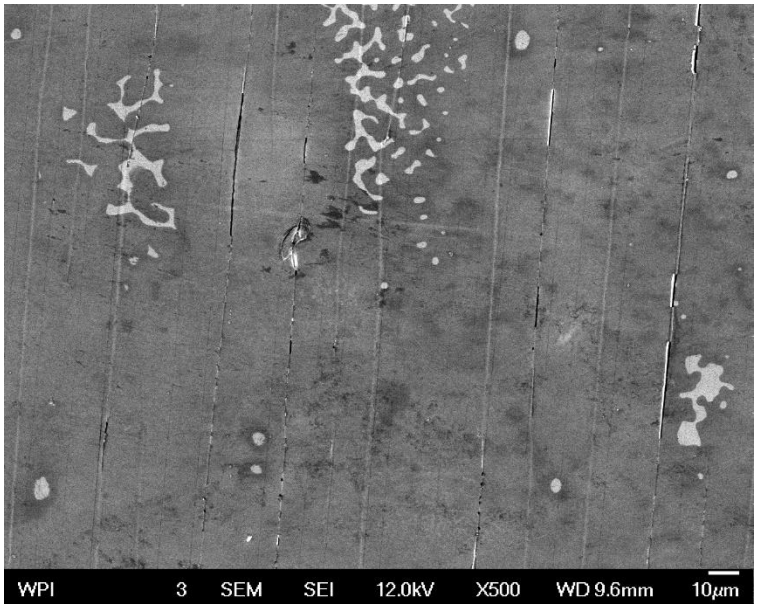

Figure 14 ITO Cracking after Bending 100 Times

We weren't all that surprised by this result, as Sigma Aldrich only advertised a max bend radius of 75 mm. This product would probably be more suitable for an application where the solar panel is fixed in place, like on a satellite or on the roof of a car. The delicate nature of ITO would prevent the use of these cells in an environment where they need to move or be bent at any extreme angle.

The Au/Pd layer proved to be somewhat more durable, only increasing in resistance by about 2.5 times at 50 bends, and 5.4 times at 100. As the resistance increase is not as bad as the ITO, this gives some hope that the Au/Pd layer might be a viable option for a flexible contact. A larger bend radius, or possibly a thinner layer, might prevent as sharp an increase in resistance, and thus the presence of cracks.

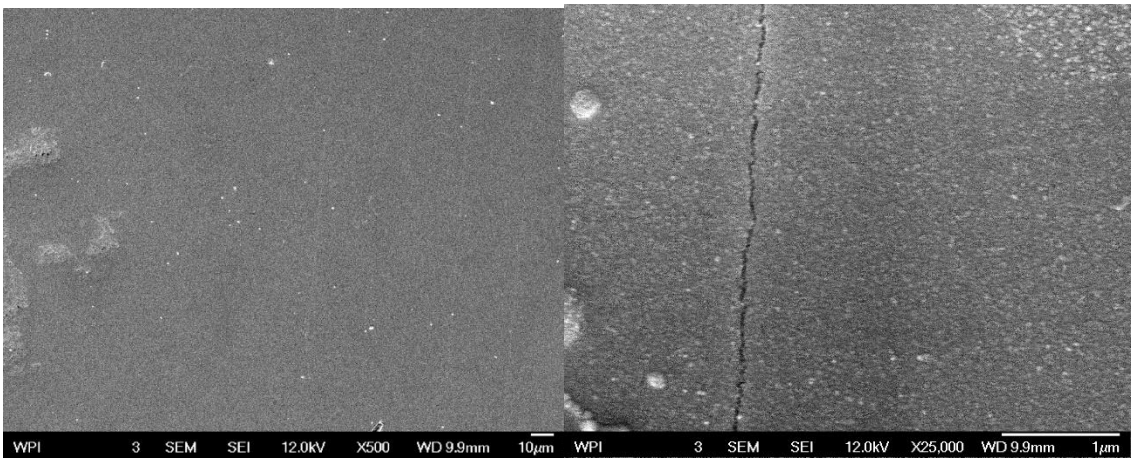

Figure 15 Cracking in Au/Pd Layer after 100 Bends

The SEM images also back up this assessment as well. The cracking in the Au/Pd layer is much less noticeable than in the ITO layer, both in the thickness and frequency of cracking.

6.2.2 TiO_2 Bending

The TiO_2 layer proved to be somewhat brittle during bending. What had started as a relatively flat and uniform surface turned into noticeably broken and cracked layer after just 50 bends.

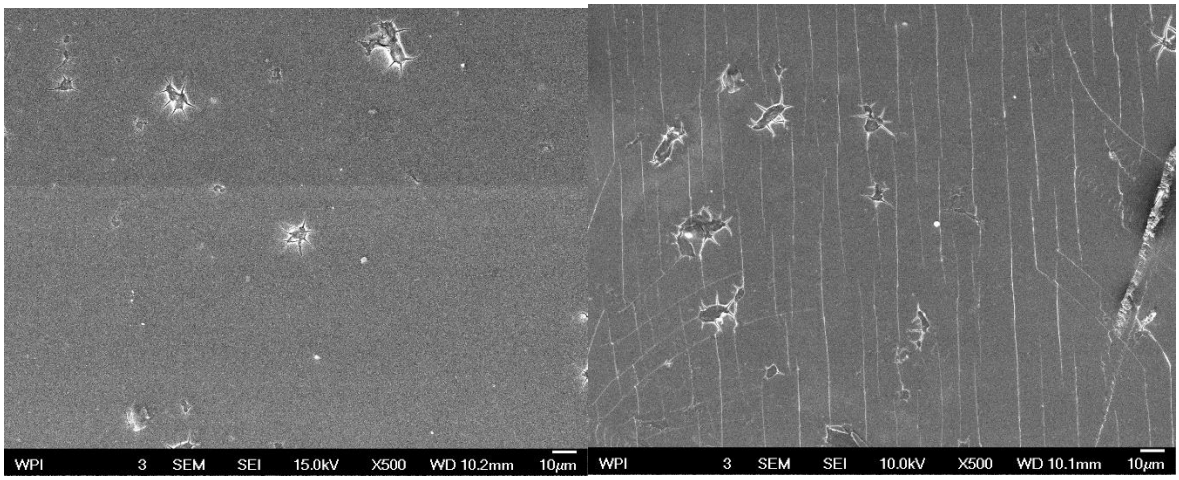

Figure 16 TiO_2 Before (Left) and After (Right) Bending 100 Times

SEM images taken from roughly the same spot show how the layer began to crack after being bent. We observed mostly vertical cracking that was in line with the axis of bending.

6.2.3 Sb2S3 Bending

The Sb_2S_3 layer was more flexible than the TiO_2 blocking layer, most likely due to the how the layer is formed of grains of Sb_2S_3.

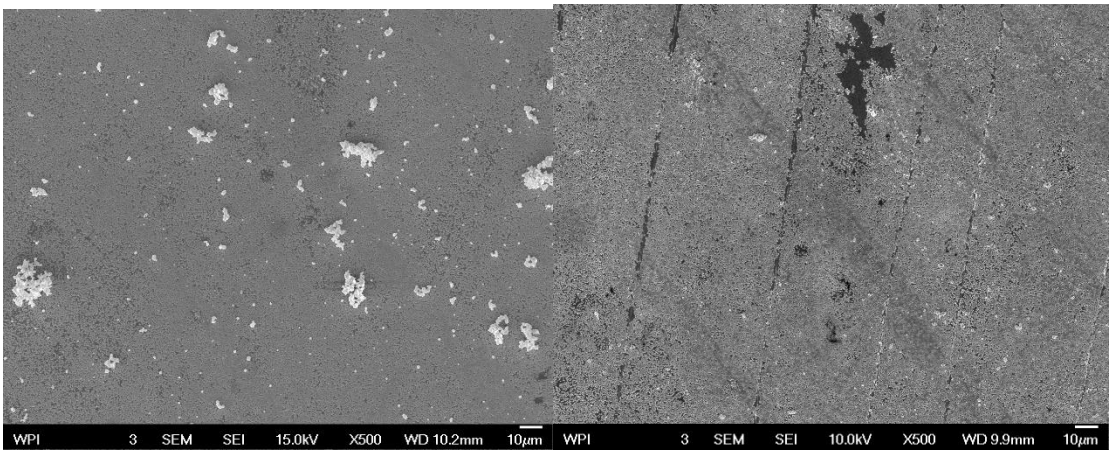

Figure 17 Sb_2S_3 Before (Left) and After (Right) Bending 100 Times

An observation that is apparent even at the scale above and becomes more obvious at small length scales is that along the vertical lines where the layer bent, the grains of Sb_2S_3 were broken off entirely. Some of the grains of the Sb_2S_3 breaking off are not detrimental to the cell like the exclusion sites on the TiO_2, but would hurt the performance of the cell nonetheless. In the picture below of Sb_2S_3 after bending it shows the missing grains along the bend, as well as, a white line going through the area of the missing grains which is evidence of the Sb_2S_3 breaking all the way through to the substrate.

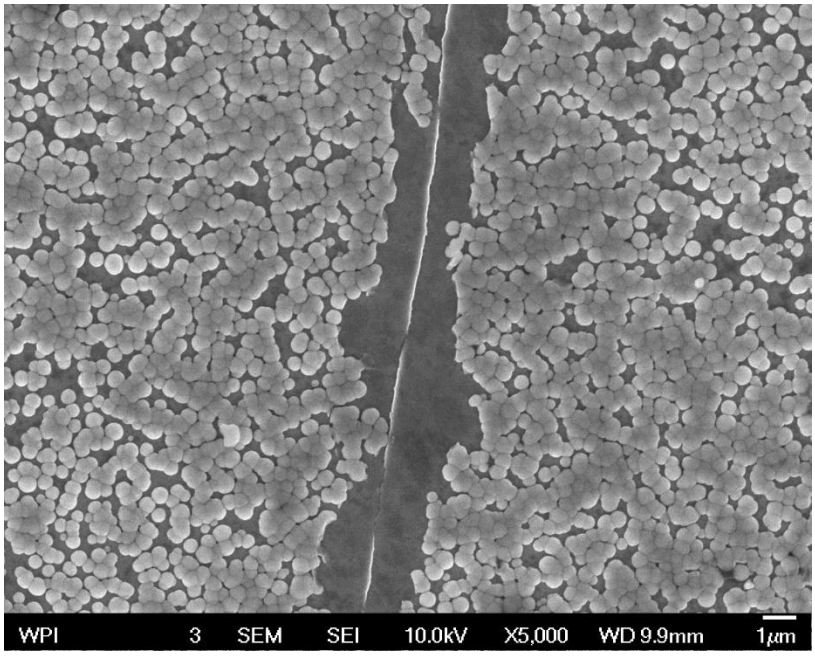

Figure 18 Valley in Sb_2S_3 Layer After Bending 100 Times

Going forward, Sb_2S_3 could see use in a flexible solar cell, as it's semi-crystalline form seems to allow a decent degree of flexibility.

6.2.4 CuSCN Bending

In the CuSCN absorber layer, we once again noticed cracking during bending as well.

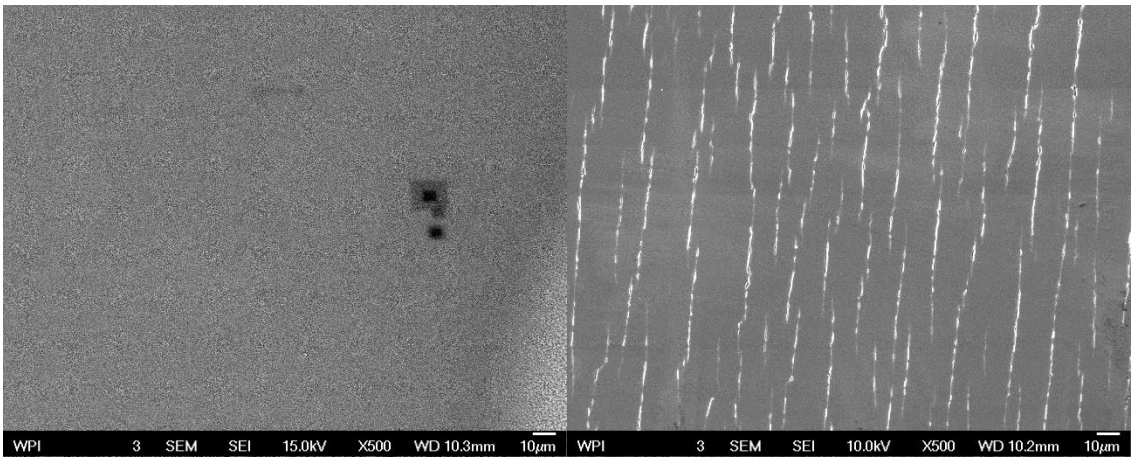

Figure 19 CuSCN Before (Left) and After (Right) Bending 100 Times

This layer produced some of the widest cracking, with cracks up to about 1 µm in width. The width of these cracks is particularly important in this layer, as the Au/Pd layer being sputtered on top of this could potentially get through these cracks and reach down to the lower layers, possibly creating a short.

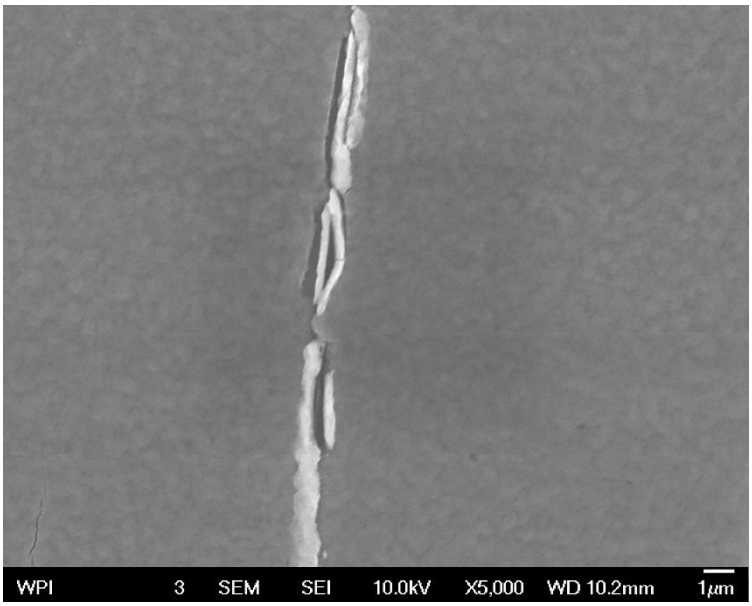

Figure 20 Large Cracking Occurring in CuSCN

These cracks could be a problem in producing a working flexible cell, as the bend radius for CuSCN may be very limited.

6.2.5 ZnO Nanowire Bending

The flexibility of the ZnO nanowires was still investigated, despite not being used in the final cell design. This was done to see what future use nanowires may have in increasing flexibility.

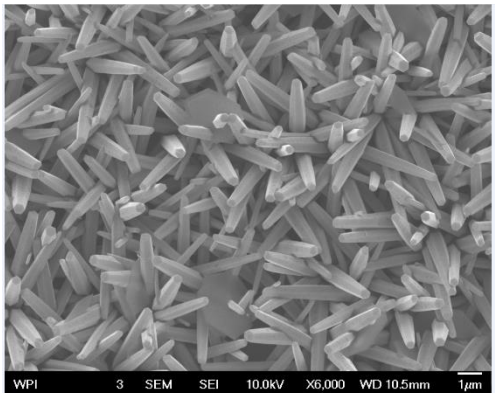

Figure 21 Close-up View of ZnO Nanowires

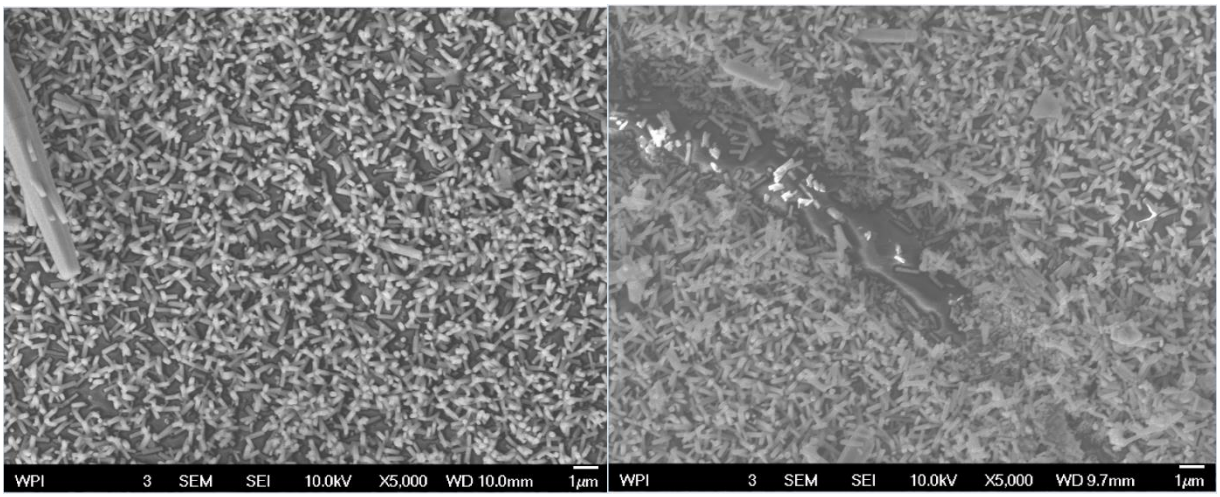

Figure 22 ZnO Nanowires Before Bending (Left)) and After Bending (Right)

As seen from the pictures in Figure 22, bending of the ZnO layers lead to valleys roughly 1 µm scale. There were far fewer of these valleys in comparison to the other layers after bending, which supports the case for the flexibility of the ZnO nanowires.

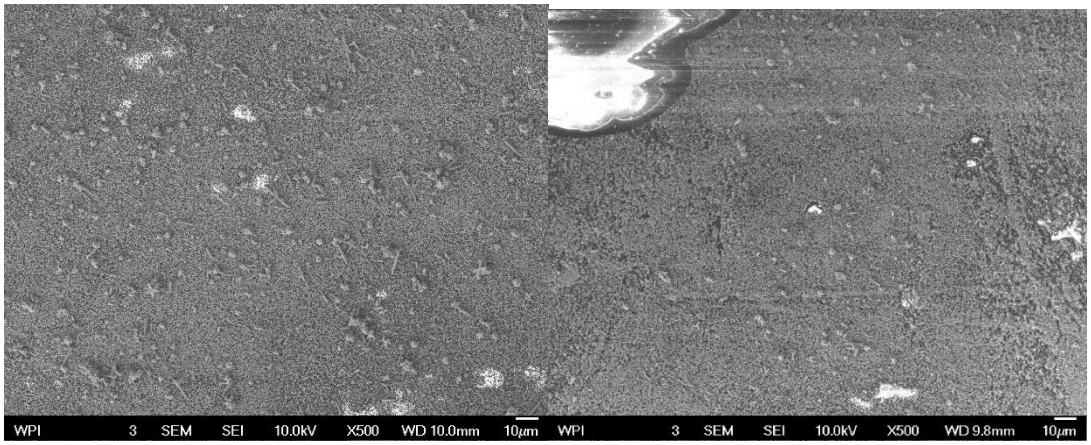

Figure 23 Macro-view of ZnO Nanowires Before (Left) and After (Right) Bending

At lower magnification levels, these valleys are far less noticeable. On the same scale, there were roughly 5 noticeable valleys in the Sb_2S_3 layer, and about 15-20 cracking lines in the TiO_2 and CuSCN layers.

We had wanted to compare the difference between vertical, ordered nanowires and the randomly oriented nanowires we produced, however, we were unable to produce the ordered nanowire structure on the PET substrate. The more orderly arrangement may allow for more movement between the nanowires, possibly improving this flexibility even more.

6.3 Low Temperature Vs. High Temperature Annealing

Comparing results between the glass and plastic substrates allowed us to see the effects that changing annealing temperatures can have. We ultimately determined that annealing was key in order to produce a decently working cell.

6.3.1 TiO_2 Annealing

High temperature annealing appears to be very important in the creation of the TiO_2 layer. Since is the blocking layer, a thick, uniform coating is important. In comparing the high temperature and low temperature annealed SEM images of this layer, we noticed that there were some large holes in the layer when annealed at the lower temperature.

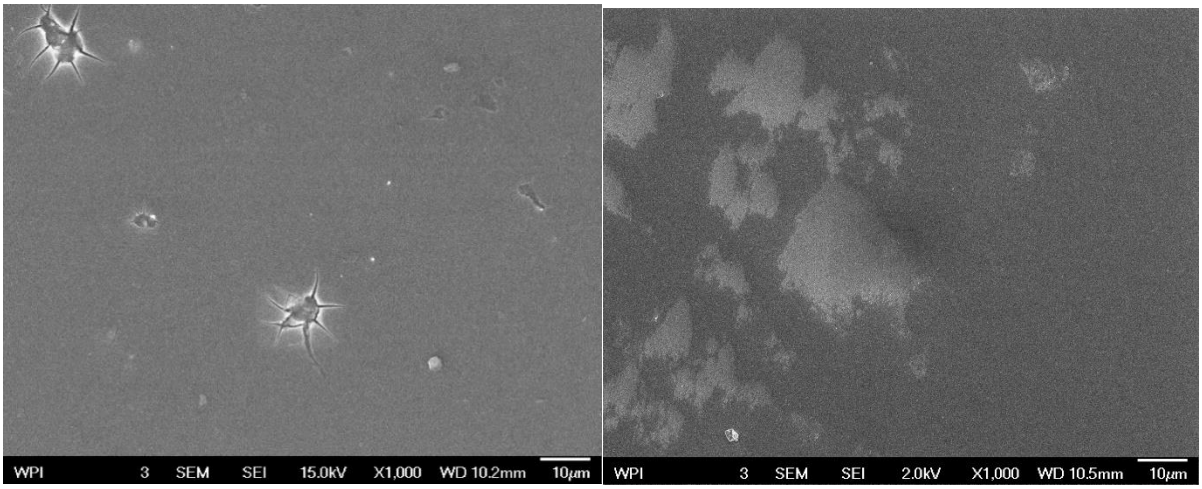

Figure 24 Low Temperature Annealed TiO_2 (Left) and High Temperature Annealed TiO_2 (Right)

As Figure 24 shows, there were holes about 5-10 μm in width in the TiO_2 layer annealed at low temperature. These holes could possibly allow for other layers to pass through the TiO_2 and touch the ITO, leading to a short. We believe these holes are caused by the propanol liquid that carries the TiO_2 solid not evaporating quickly enough, leaving puddles of liquid that create these holes when the liquid does finally evaporate. The image of TiO_2 on the right in Figure 24 is what the layer should look like, as a uniform layer with no apparent porosity.

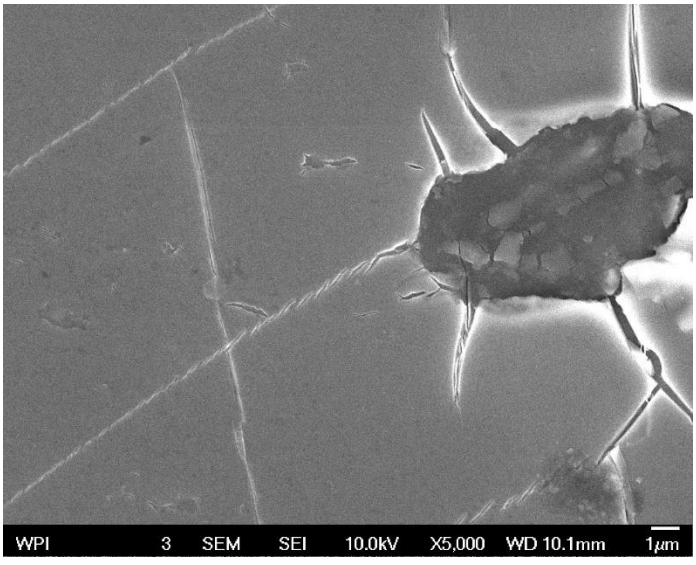

Figure 25 Cracking Initiated by Holes in TiO_2 Layer

Besides the possible shorts that these holes can lead to, they also facilitate cracking when the cell is bent. During the bending tests mentioned previously, we noted that there was some vertical and

horizontal cracking propagating off these holes. While there was plenty of cracking regardless, these holes seem to have made the problem worse.

6.3.2 Sb_2S_3 Annealing

As observed in the Sb_2S_3 bending tests, the un-annealed form appears to be quite flexible. However, it seems that the layer works better in terms of solar efficiency when it has been annealed at high temperatures. We tried testing cells with just low temperature annealed Sb_2S_3 on them, which should be enough to produce a working cell, but always produced a non-responsive cell.

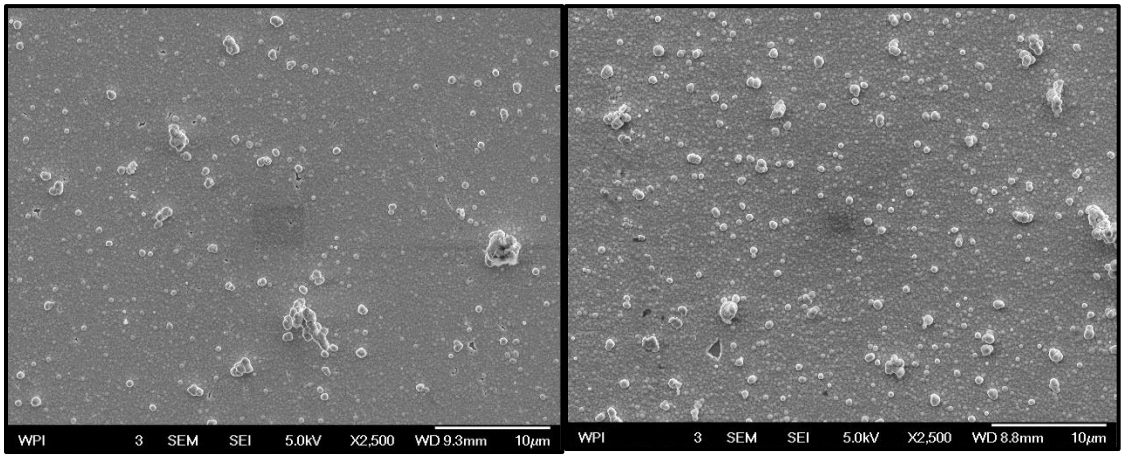

Figure 26 Annealed Sb_2S_3 (Left) and Un-annealed Sb_2S_3 (Right)

Looking at the two SEM images, we can see the difference between the annealed and un-annealed Sb_2S_3. The annealed Sb_2S_3 has a much more uniform surface, with fewer of the grain overgrowths. There are also some slight holes in the un-annealed Sb_2S_3 layer, roughly 1-2 μm in size.

7. Recommendations

As this MQP will be continued next year, we will lay out some of the recommendations that we have for future students working on this project.

7.1 ZnO Layer

We managed to achieve nanowire growth on our plastic substrate, but were not able to produce the dense layer that we had hoped to use as a blocking layer. The nanowires appear to be quite flexible, as illustrated in the above section, so they could possibly be used to increase the flexibility of the less flexible layers. ZnO nanowires appeared to have dissolved in the Sb_2S_3 bath however, so either a different nanowire material or different absorber layer may be needed. The bath for Sb_2S_3 has a pH of roughly 5, so the acidity of this bath may be the reason for the dissolution of the nanowires.[57]

7.2 TiO_2 Layer

We had some concerns during this project that the low temperature annealing for TiO_2 might not have been producing a dense enough layer. Annealing at low temperatures most likely left the TiO_2 layer in an amorphous state, which could have allowed other layers to penetrate it. To combat this, we had hoped to try creating the TiO_2 layer using TiO_2 paste via screen printing, as opposed to spin coating the liquid TiO_2. The paste would have had fully annealed TiO_2 crystals within it, thus giving us a better chance at producing a dense blocking layer. Unfortunately, the paste would not have arrived in time for us to test this theory.

7.3 Sb_2S_3 Layer

The main concern with the Sb_2S_3 were the extra growths that occurred atop the surface. These growths may have interfered with the CuSCN layer and affected the performance of the cell. One possible solution that we found for this was to use dry Acetone in the solution. The dry Acetone only has 0.0075% water within it. The reduced water content should allow for a cleaner reaction, hopefully limiting the amount of overgrowths present on the surface. We also found that annealing the Sb_2S_3 in nitrogen produced a much better layer, however, this is not feasible on the PET substrate.

SEM EDS of the Sb_2S_3 was conducted to investigate if the overgrowths on the layer were the same material as the main layer or an antimony oxide that may be hurting the cell performance.

[57] (Nair et al., 1998)

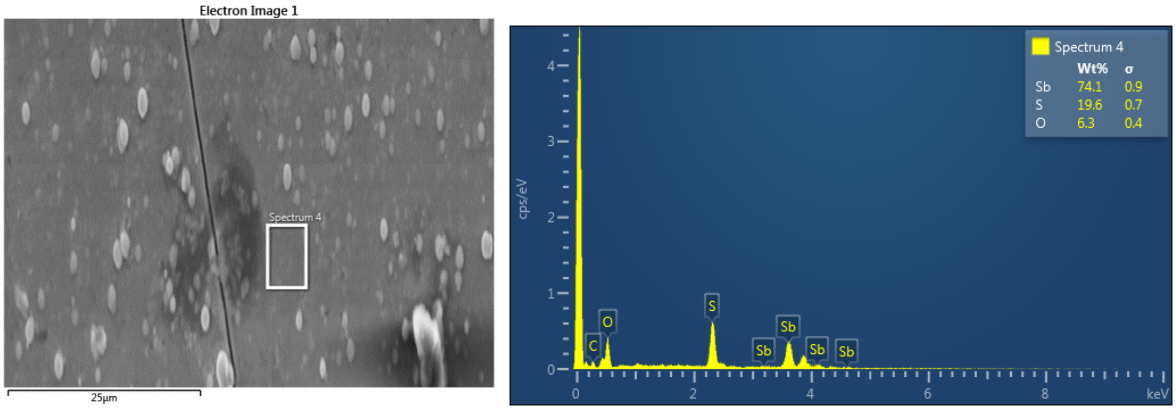

Figure 27 SEM EDS of the Sb_2S_3 Layer for Comparison

In the first part of the test we took data from a section of the Sb_2S_3 layer had no overgrowths and took a reading of the weight percent of each element of the material there. The read out we got from this test showed that the material was 74.1 Wt% Sb, 19.6 Wt% S, and 6.3 Wt% O, with the oxygen coming from the remnants of the Sodium Thiocyanate, $Na_2S_2O_3$, from the reaction.

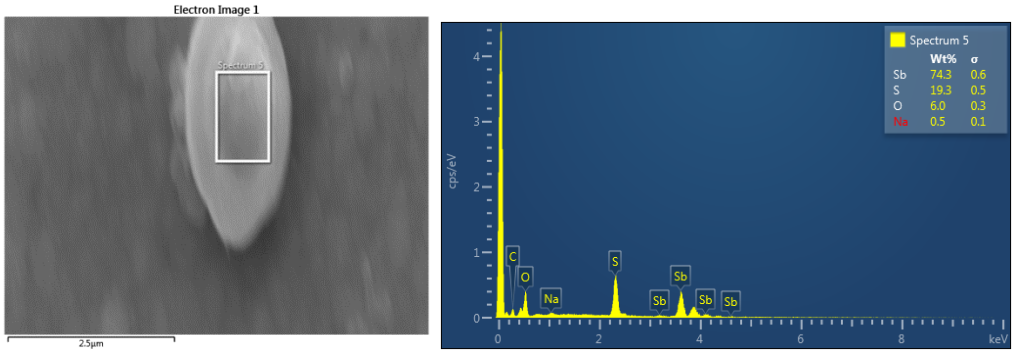

Figure 28 SEM EDS of Sb_2S_3 Growth

In the second part of the test we zoomed in on one of the overgrowths and took a reading of the weight percent of each element of the material there. The reading we got from this test showed that the material was 74.3 Wt% Sb, 19.3 Wt% S, and 6.0 Wt% O, and 0.5 Wt% Na. This is essentially the same weight percents as the main layer, confirming that it is not another material that could hurt the cells performance. The presence of Na in this is not a cause for concern because the text specifying the element is red, indicating that the program was unsure about the presence of this element. If Na is present on that section of the layer it would again be a result of left over Sodium Thiocyanate from the previous reaction.

7.4 Substrate and Electrodes

One possible solution to some of the problems we ran into would be changing the substrate the cell is based on. PET greatly limits the annealing temperature, which impacts many of the layers in the cell. Either finding a different, more robust plastic substrate that can withstand higher temperatures, or using a flexible metal substrate. Using aluminum foil, for example, as the back contact for the cell would allow for high temperature annealing, while maintaining a degree of flexibility. The downside to this approach will be the clear conductive layer, as depositing this layer will not be as simple as some of the other layers in the cell. For example, the ITO layered on our PET substrate was done via sputtering ITO, something that we cannot do in lab. A different transparent conductive layer would need to be investigated.

The gold contact should also be more closely examined as the thinness of the gold palladium mixture may have led to a larger resistivity than expected. The gold contact was delicate and would peel off when the copper tape attachments were removed as well. The copper tape contact could also be explored, as the connection between the copper tape and the cell itself didn't seem to be as good as it could be. A more secure connection between the cell and the test leads could improve the efficiency.

8. Conclusions

This study showed us that the combination of PET, ITO, Sb_2S_3, CuSCn, and gold/palladium is a viable flexible solar cell that should be studied in more depth to increase the efficiency of the cell. Other material options, material deposition processes, and cell designs should also be explored to attempt to create a more resilient solar cell.

To perform many of the processes that were involved in the creation of these cells our group had to work together to plan and schedule. Often with our work there were setbacks in the laboratory that would delay us for days. Other times when we were met with several failures in a row we had to learn to innovate and overcome the obstacle we faced. Learning to work with other people outside of our group was also important, as we relied on the help of graduate students for learning lab practices and for obtaining SEM images. With proper planning and communication, we were able to work very well together.

Creating flexible solar cells is an important step in the future of the energy industry. The applications of solar power will be greatly increased with the advancement and implementation of flexible solar cells.

Appendix A

The following is a list of terminology that is used throughout the paper.

Material Structure:

Amorphous: Without a defined structure, pertaining to the structure of the material

Mono/Polycrystalline: Having a organized, repeating structure. In monocrystalline structure a single crystal structure is repeated where in polycrystalline different crystal structures exist.

Doping: Adding Impurities to a material to encourage charge movement

Blend composition: Pertaining to the materials that make up a BHJ cell

X ray diffraction: The process of using an X ray machine to study material properties

3D morphology: The study of the geometry of the P/N layers in a bulk heterojunction cell

Electron tomography: A machine that is used to study material properties

Solar Cell Structure:

Multi-junction: A solar cell having more than one P/N layer for better absorption characteristics

Substrate: The material that the different cell layers are built up on

P/N Semiconductors: The central layers of a solar cell that create the movement of electrons to form a circuit because of photons hitting the solar cell

Anti-reflective: Coating that prevents light from reflecting back into the air

Nanowires: See Nanowires

Conductive layers: Outer layers of a cell that completes circuit of solar cell connecting P/N layers to the grid

Manufacturing:

Roll to Roll Manufacturing: Type of manufacturing where electronics are printed onto substrate through a series of rollers that move the substrate continuously

Vacuum Deposition: See vapor deposition

Chemical Bath Deposition: See chemical bath deposition

Other Terms:

Power Point: Operating voltage and current which produce maximum power

AM1: Sun illumination intensity on a clear day at noon

Fill factor: Maximum power that can be derived from solar cell

Appendix B

Materials	Cell Types
Alkaline manganese batteries Aluminum conductive layers Al/ZnO reflector a-SiG alloy photovoltaics BHJ (inkjet) Bi_2S_3 Ca Cadmium Sulfide (CdS) Carbon Nanotubes (CNT) Cu (wires) FTO Fullerene GMS (glycerol monostearate) Graphene ITO conductive layer ITO-ZnO LiF/AL Contact MoO_3 Ohmic Contacts Oxide-metal-oxide multilayers P3HT:PCBM PCDTBT:PCBM PEDOT:PSS Perovskite PET, PES, PEN substrates Photovoltaic Inks Sb_2S_3 Silver nanowires Stainless steel substrate TiO_2	a-S BIPV Bulk Heterojunction (BHJ) CdTe CIGS/CIS c-SI (mono vs poly) DSSCs Organic Perovskite Polymer Thin Film

Works Cited

Amorphous Silicon Solar Panels. (2013). Retrieved from http://www.solar-facts-and-advice.com/amorphous-silicon.html

Bach, U., Lupo, D., Comte, P., Moser, J. E., Weissortel, F., Salbeck, J., . . . Gratzel, M. (1998). Solid-state dye-sensitized mesoporous TiO2 solar cells with high photon-to-electron conversion efficiencies. *Nature, 395*(6702), 583-585.

Brabec, C. J., Gowrisanker, S., Halls, J. J. M., Laird, D., Jia, S., & Williams, S. P. (2010). Polymer–Fullerene Bulk-Heterojunction Solar Cells. *Advanced Materials, 22*(34), 3839-3856. doi:10.1002/adma.200903697

Brusdeylins, C. (2016). ZSW Sets New World Record for Thin-film Solar Cells [Press release]. Retrieved from https://www.zsw-bw.de/fileadmin/user_upload/PDFs/Pressemitteilungen/2016/pr09-2016-ZSW-WorldRecordCIGS.pdf

Cadmium Telluride. (2016). Retrieved from http://www.energy.gov/eere/sunshot/cadmium-telluride

Chandiran, A. K., Yella, A., Mayer, M. T., Gao, P., Nazeeruddin, M. K., & Grätzel, M. (2014). Sub-Nanometer Conformal TiO2 Blocking Layer for High Efficiency Solid-State Perovskite Absorber Solar Cells. *Advanced Materials, 26*(25), 4309-4312. doi:10.1002/adma.201306271

Chen, L., Lai, J. S., Fu, X. N., Sun, J., Ying, Z. F., Wu, J. D., . . . Xu, N. (2013). Growth of ZnSe nano-needles by pulsed laser deposition and their application in polymer/inorganic hybrid solar cells. *Thin Solid Films, 529*, 76-79. doi:http://dx.doi.org/10.1016/j.tsf.2012.02.037

Choi, K.-H., Kim, J., Noh, Y.-J., Na, S.-I., & Kim, H.-K. (2013). Ag nanowire-embedded ITO films as a near-infrared transparent and flexible anode for flexible organic solar cells. *Solar Energy Materials and Solar Cells, 110*, 147-153. doi:http://dx.doi.org/10.1016/j.solmat.2012.12.022

Choubey, R. K., Desai, D., Kale, S. N., & Kumar, S. (2016). Effect of annealing treatment and deposition temperature on CdS thin films for CIGS solar cells applications. *Journal of Materials Science: Materials in Electronics, 27*(8), 7890-7898. doi:10.1007/s10854-016-4780-2

De Bettignies, R., Leroy, J., Firon, M., & Sentein, C. (2006). Accelerated lifetime measurements of P3HT:PCBM solar cells. *Synthetic Metals, 156*(7–8), 510-513. doi:http://dx.doi.org/10.1016/j.synthmet.2005.06.016

De Volder, M. F. L., Tawfick, S. H., Baughman, R. H., & Hart, A. J. (2013). Carbon Nanotubes: Present and Future Commercial Applications. *Science, 339*(6119), 535-539. doi:10.1126/science.1222453

Dume, B. (2012). Doped Nanotubes Make Transparent Electrodes. Retrieved from http://nanotechweb.org/cws/article/tech/50250

Englman, T., Terkieltaub, E., & Etgar, L. (2015). High Open Circuit Voltage in Sb2S3/Metal Oxide-Based Solar Cells. *The Journal of Physical Chemistry C, 119*(23), 12904-12909. doi:10.1021/acs.jpcc.5b04231

Erb, T., Zhokhavets, U., Gobsch, G., Raleva, S., Stühn, B., Schilinsky, P., . . . Brabec, C. J. (2005). Correlation Between Structural and Optical Properties of Composite Polymer/Fullerene Films for Organic Solar Cells. *Advanced Functional Materials, 15*(7), 1193-1196. doi:10.1002/adfm.200400521

Greene, L. E., Law, M., Tan, D. H., Montano, M., Goldberger, J., Somorjai, G., & Yang, P. (2005). General Route to Vertical ZnO Nanowire Arrays Using Textured ZnO Seeds. *Nano Letters, 5*(7), 1231-1236. doi:10.1021/nl050788p

Grätzel, M. (2011). Dye-Sensitized Solid-State Heterojunction Solar Cells. *MRS Bulletin, 30*(1), 23-27. doi:10.1557/mrs2005.4

Haeussler, M. (2009). Fabrication of Organic Photovoltaic Devices. Retrieved from http://www.azonano.com/article.aspx?ArticleID=2434

Heo, J. H., Im, S. H., Noh, J. H., Mandal, T. N., Lim, C.-S., Chang, J. A., . . . Seok, S. I. (2013). Efficient inorganic-organic hybrid heterojunction solar cells containing perovskite compound and polymeric hole conductors. *Nat Photon, 7*(6), 486-491. doi:10.1038/nphoton.2013.80

http://www.nature.com/nphoton/journal/v7/n6/abs/nphoton.2013.80.html#supplementary-information

Hwang, J., Shoji, N., Endo, A., & Daiguji, H. (2014). Effect of Withdrawal Speed on Film Thickness and Hexagonal Pore-Array Dimensions of SBA-15 Mesoporous Silica Thin Film. *Langmuir, 30*(51), 15550-15559. doi:10.1021/la5037713

Hyesung Park and Jill, A. R. a. K. K. K. a. V. B. a. J. K. (2010). Doped graphene electrodes for organic solar cells. *Nanotechnology, 21*(50), 505204.

Itzhaik, Y., Niitsoo, O., Page, M., & Hodes, G. (2009). Sb2S3-Sensitized Nanoporous TiO2 Solar Cells. *The Journal of Physical Chemistry C, 113*(11), 4254-4256. doi:10.1021/jp900302b

Jagadamma, L. K., Abdelsamie, M., El Labban, A., Aresu, E., Ngongang Ndjawa, G. O., Anjum, D. H., . . . Amassian, A. (2014). Efficient inverted bulk-heterojunction solar cells from low-temperature processing of amorphous ZnO buffer layers. *Journal of Materials Chemistry A, 2*(33), 13321-13331. doi:10.1039/C4TA02276A

Junghänel, M. (2007). *Novel Aqueous Electrolyte Films for Hole Conduction in Dye Sensitized Solar Cells and Development of an Electron Transport Model*. In. Retrieved from http://www.diss.fu-berlin.de/diss/servlets/MCRFileNodeServlet/FUDISS_derivate_000000002568/02_2.pdf?hosts

Kumara, G. R. R. A., Konno, A., Senadeera, G. K. R., Jayaweera, P. V. V., De Silva, D. B. R. A., & Tennakone, K. (2001). Dye-sensitized solar cell with the hole collector p-CuSCN deposited from a solution in n-propyl sulphide. *Solar Energy Materials and Solar Cells, 69*(2), 195-199. doi:http://dx.doi.org/10.1016/S0927-0248(01)00027-7

Law, M., Greene, L. E., Johnson, J. C., Saykally, R., & Yang, P. (2005). Nanowire dye-sensitized solar cells. *Nat Mater, 4*(6), 455-459. doi:http://www.nature.com/nmat/journal/v4/n6/suppinfo/nmat1387_S1.html

Li, X., Bi, D., Yi, C., Décoppet, J.-D., Luo, J., Zakeeruddin, S. M., . . . Grätzel, M. (2016). A vacuum flash–assisted solution process for high-efficiency large-area perovskite solar cells. *Science, 353*(6294), 58-62. doi:10.1126/science.aaf8060

Malinkiewicz, O., Yella, A., Lee, Y. H., Espallargas, G. M., Graetzel, M., Nazeeruddin, M. K., & Bolink, H. J. (2014). Perovskite solar cells employing organic charge-transport layers. *Nat Photon, 8*(2), 128-132. doi:10.1038/nphoton.2013.341

http://www.nature.com/nphoton/journal/v8/n2/abs/nphoton.2013.341.html#supplementary-information

MiaSolé Product Page. (2016). Retrieved from http://miasole.com/products/

Minami, T. (2008). Present status of transparent conducting oxide thin-film development for Indium-Tin-Oxide (ITO) substitutes. *Thin Solid Films, 516*(17), 5822-5828. doi:http://dx.doi.org/10.1016/j.tsf.2007.10.063

Moon, S.-J., Itzhaik, Y., Yum, J.-H., Zakeeruddin, S. M., Hodes, G., & Grätzel, M. (2010). Sb2S3-Based Mesoscopic Solar Cell using an Organic Hole Conductor. *The Journal of Physical Chemistry Letters, 1*(10), 1524-1527. doi:10.1021/jz100308q

Nair, M. T. S., Pena, Y., Campos, J., Garcia, V. M., & Nair, P. K. (1998). Chemically Deposited Sb2 S 3 and Sb2 S 3-CuS Thin Films. *Journal of The Electrochemical Society, 145*(6), 2113-2120.

Nostell, P., Roos, A., & Karlsson, B. (1999). Optical and mechanical properties of sol-gel antireflective films for solar energy applications. *Thin Solid Films, 351*(1–2), 170-175. doi:http://dx.doi.org/10.1016/S0040-6090(99)00257-6

O'Regan, B., & Schwartz, D. T. (1995). Efficient Photo-Hole Injection from Adsorbed Cyanine Dyes into Electrodeposited Copper(I) Thiocyanate Thin Films. *Chemistry of Materials, 7*(7), 1349-1354. doi:10.1021/cm00055a012

Pineda, E., Nicho, M. E., Nair, P. K., & Hu, H. (2012). Optoelectronic properties of chemically deposited Bi2S3 thin films and the photovoltaic performance of Bi2S3/P3OT solar cells. *Solar Energy, 86*(4), 1017-1022. doi:http://dx.doi.org/10.1016/j.solener.2011.06.015

Qu, J., Yang, Y., Wu, Q., Coxon, P. R., Liu, Y., He, X., . . . Ding, J. (2014). Hedgehog-like hierarchical ZnO needle-clusters with superior electron transfer kinetics for dye-sensitized solar cells. *RSC Advances, 4*(22), 11430-11437.

Rath, A. K., Bernechea, M., Martinez, L., & Konstantatos, G. (2011). Solution-Processed Heterojunction Solar Cells Based on p-type PbS Quantum Dots and n-type Bi2S3 Nanocrystals. *Advanced Materials, 23*(32), 3712-3717. doi:10.1002/adma.201101399

Roldán-Carmona, C., Malinkiewicz, O., Soriano, A., Espallargas, G. M., Garcia, A., Reinecke, P., . . . Bolink, H. J. (2014). Flexible high efficiency perovskite solar cells. *Energy & Environmental Science, 7*(3), 994-997.

Roll to Roll (R2R) Processing Technology Assessment. (2015). In: US Department of Energy.

Sahu, N., Parija, B., & Panigrahi, S. (2009). Fundamental understanding and modeling of spin coating process: A review. *Indian Journal of Physics, 83*(4), 493-502. doi:10.1007/s12648-009-0009-z

Salunkhe, D. B., Dubal, D. P., Sali, J. V., & Sankapal, B. R. (2015). Linker free synthesis of TiO2/Bi2S3 heterostructure towards solar cell application: Facile chemical routes. *Materials Science in Semiconductor Processing, 30*, 335-342. doi:http://dx.doi.org/10.1016/j.mssp.2014.10.024

Scharber, M. C. (2016). On the Efficiency Limit of Conjugated Polymer:Fullerene-Based Bulk Heterojunction Solar Cells. *Advanced Materials, 28*(10), 1994-2001. doi:10.1002/adma.201504914

Stanbery, B. J. (2002). Copper Indium Selenides and Related Materials for Photovoltaic Devices. *Critical Reviews in Solid State and Materials Sciences, 27*(2), 73-117. doi:10.1080/20014091104215

Tanveer, M., Habib, A., & Khan, M. B. (2012). Improved efficiency of organic/inorganic photovoltaic devices by electrospun ZnO nanofibers. *Materials Science and Engineering: B, 177*(13), 1144-1148. doi:http://dx.doi.org/10.1016/j.mseb.2012.05.025

University of Florida, U. O. L. Spin Coating. In: University of Florida.

van Bavel, S. S., Bärenklau, M., de With, G., Hoppe, H., & Loos, J. (2010). P3HT/PCBM Bulk Heterojunction Solar Cells: Impact of Blend Composition and 3D Morphology on Device Performance. *Advanced Functional Materials, 20*(9), 1458-1463. doi:10.1002/adfm.200902247

Wang, W.-W., & Zhu, Y.-J. (2004). Synthesis of Needle-like and Flower-like Zinc Oxide by a Simple Surfactant-free Solution Method. *Chemistry Letters, 33*(8), 988-989. doi:10.1246/cl.2004.988

Wang, Y., Tong, S. W., Xu, X. F., Özyilmaz, B., & Loh, K. P. (2011). Interface Engineering of Layer-by-Layer Stacked Graphene Anodes for High-Performance Organic Solar Cells. *Advanced Materials, 23*(13), 1514-1518. doi:10.1002/adma.201003673

Wang, Z., Qian, X.-f., Yin, J., & Zhu, Z.-k. (2004). Large-Scale Fabrication of Tower-like, Flower-like, and Tube-like ZnO Arrays by a Simple Chemical Solution Route. *Langmuir, 20*(8), 3441-3448. doi:10.1021/la036098n

Wenas, W. W., Yamada, A., Takahashi, K., Yoshino, M., & Konagai, M. (1991). Electrical and optical properties of boron-doped ZnO thin films for solar cells grown by metalorganic chemical vapor deposition. *Journal of Applied Physics, 70*(11), 7119-7123. doi:doi:http://dx.doi.org/10.1063/1.349794

Yaacobi-Gross, N., Treat, N. D., Pattanasattayavong, P., Faber, H., Perumal, A. K., Stingelin, N., . . . Anthopoulos, T. D. (2015). High-Efficiency Organic Photovoltaic Cells Based on the Solution-

Processable Hole Transporting Interlayer Copper Thiocyanate (CuSCN) as a Replacement for PEDOT:PSS. *Advanced Energy Materials, 5*(3), 1401529-n/a. doi:10.1002/aenm.201401529

Yang, L., Zhang, T., Zhou, H., Price, S. C., Wiley, B. J., & You, W. (2011). Solution-Processed Flexible Polymer Solar Cells with Silver Nanowire Electrodes. *ACS Applied Materials & Interfaces, 3*(10), 4075-4084. doi:10.1021/am2009585

Zhang, W., Zhao, B., He, Z., Zhao, X., Wang, H., Yang, S., . . . Cao, Y. (2013). High-efficiency ITO-free polymer solar cells using highly conductive PEDOT: PSS/surfactant bilayer transparent anodes. *Energy & Environmental Science, 6*(6), 1956-1964.